

# Machinery fault diagnosis using vibration analysis

## 5.1 Introduction

Present day requirements for enhanced reliability of rotating equipment are more critical than ever before, and the demands continue to grow constantly. Advances are constantly made in this area, largely due to the consistent demand from the hydrocarbon, power-generation, process and transportation industries.

Due to the progress made in engineering and materials science, rotating machinery is becoming faster and lightweight. They are also required to run for longer periods of time. All of these factors mean that the detection, location and analysis of faults play a vital role in the quest for highly reliable operations.

Using vibration analysis, the condition of a machine can be constantly monitored. Detailed analyses can be made to determine the health of a machine and identify any faults that may be arising or that already exist.

In this chapter, further attention is given to the method of correlating rotating machine defects to vibrations collected and displayed by the various types of analyzers.

## 5.2 Commonly witnessed machinery faults diagnosed by vibration analysis

Some of the machinery defects detected using vibration analysis are listed below:

- Unbalance
- Bent shaft
- Eccentricity
- Misalignment
- Looseness
- Belt drive problems
- Gear defects
- Bearing defects
- Electrical faults
- Oil whip/whirl
- Cavitation
- Shaft cracks

- Rotor rubs
- Resonance
- Hydraulic and aerodynamic forces.

We will now look at each one of the above cases in detail and see how they manifest in vibration analysis.

### 5.2.1 Unbalance

Vibration due to unbalance of a rotor is probably the most common machinery defect. It is luckily also very easy to detect and rectify. The International Standards Organisation (ISO) define unbalance as:

*That condition, which exists in a rotor when vibratory, force or motion is imparted to its bearings as a result of centrifugal forces.*

It may also be defined as: *The uneven distribution of mass about a rotor's rotating centerline.*

There are two new terminologies used: one is *rotating centerline* and the other is *geometric centerline*.

The *rotating centerline* is defined as the axis about which the rotor would rotate if not constrained by its bearings (also called the principle inertia axis or PIA).

The *geometric centerline* (GCL) is the physical centerline of the rotor.

When the two centerlines are coincident, then the rotor will be in a state of balance. When they are apart, the rotor will be unbalanced. There are three types of unbalance that can be encountered on machines, and these are:

1. Static unbalance (PIA and GCL are parallel)
2. Couple unbalance (PIA and GCL intersect in the center)
3. Dynamic unbalance (PIA and GCL do not touch or coincide).

#### Static unbalance

For all types of unbalance, the FFT spectrum will show a predominant  $1 \times \text{rpm}$  frequency of vibration. Vibration amplitude at the  $1 \times \text{rpm}$  frequency will vary proportional to the square of the rotational speed. It is always present and normally dominates the vibration spectrum (Figure 5.1).

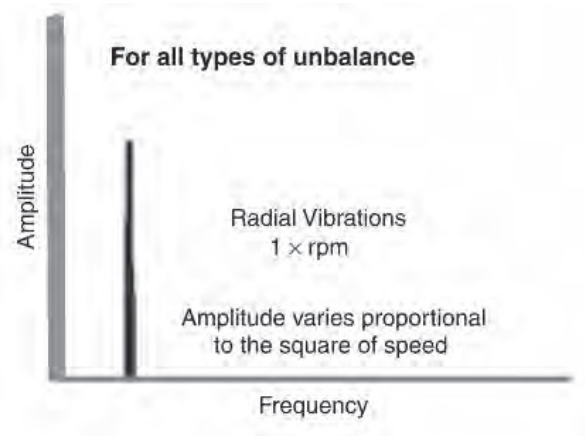


**Figure 5.1**  
*FFT analysis – unbalance defect*

Static unbalance will be in-phase and steady ( $15\text{--}20^\circ$ ). If the pickup is moved from the vertical (V in the figure) direction to the horizontal (H in the figure) direction, the phase will shift by  $90^\circ$  ( $\pm 30^\circ$ ). Another test is to move the pickup from one bearing to another in the same plane (vertical or horizontal). The phase will remain the same, if the fault is static unbalance (Figure 5.2).

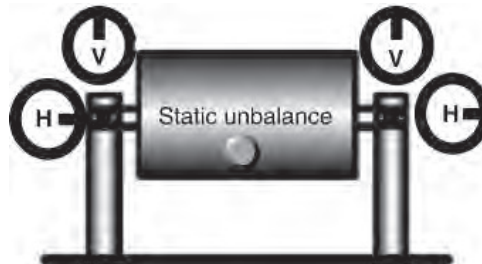


**Figure 5.2**  
*Phase relationship – static unbalance*

If the machine has no other major defects besides unbalance, the time waveform will be a clean SHM waveform with the frequency the same as the running speed.

### Couple unbalance

In a couple unbalance (Figure 5.3) the FFT spectrum again displays a single  $1\times$  rpm frequency peak. The amplitude at the  $1\times$  varies proportional to the square of speed. This defect may cause high axial and radial vibrations. Couple unbalance tends to be  $180^\circ$  out of phase on the same shaft. Note that almost a  $180^\circ$  phase difference exists between two bearings in the horizontal plane. The same is observed in the vertical plane. It is advisable to perform an operational deflection shape (ODS) analysis to check if couple unbalance is present in a system.

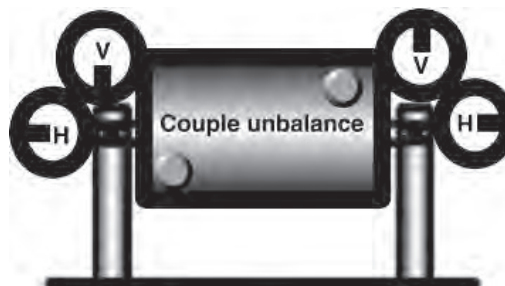


**Figure 5.3**  
*Phase relationship – couple unbalance*

### Unbalance – overhung rotors

In this case, the FFT spectrum displays a single  $1\times$  rpm peak as well, and the amplitude again varies proportional to the square of the shaft speed. It may cause high axial and radial vibrations. The axial phase on the two bearings will seem to be in phase whereas

the radial phase tends to be unsteady. Overhung rotors can have both static and couple unbalance and must be tested and fixed using analyzers or balancing equipment (Figure 5.4).

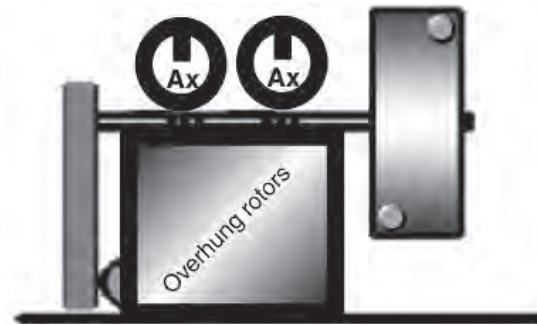


**Figure 5.4**

*A belt-driven fan/blower with an overhung rotor – the phase is measured in the axial direction*

## 5.2.2 Eccentric rotor

Eccentricity occurs when the center of rotation is at an offset from the geometric centerline of a sheave, gear, bearing, motor armature or any other rotor. The maximum amplitude occurs at  $1\times$  rpm of the eccentric component in a direction through the centers of the two rotors. Here the amplitude varies with the load even at constant speeds (Figure 5.5).

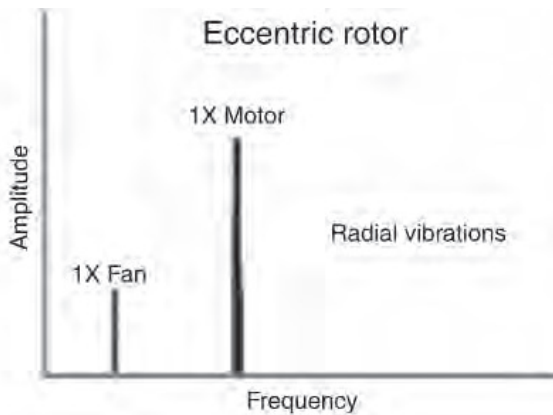


**Figure 5.5**

*A belt-driven fan/blower – vibration graph*

In a normal unbalance defect, when the pickup is moved from the vertical to the horizontal direction, a phase shift of  $90^\circ$  will be observed. However in eccentricity, the phase readings differ by  $0$  or  $180^\circ$  (each indicates straight-line motion) when measured in the horizontal and vertical directions. Attempts to balance an eccentric rotor often result in reducing the vibration in one direction, but increasing it in the other radial direction (depending on the severity of the eccentricity) (Figure 5.6).

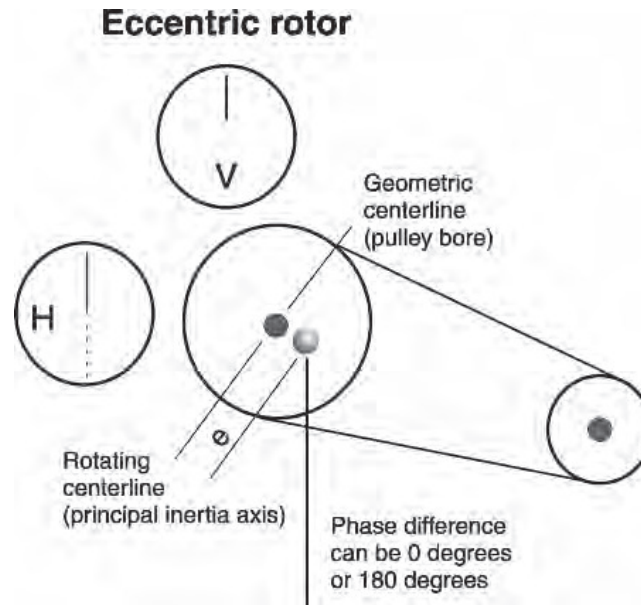
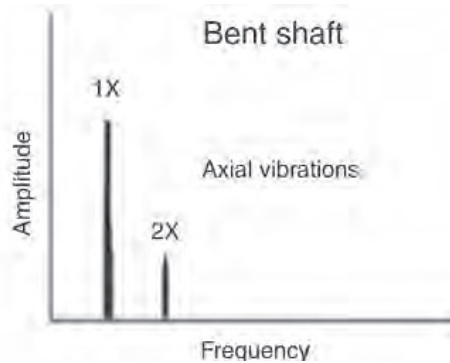


**Figure 5.6**  
*Eccentric rotor*

### 5.2.3 Bent shaft

When a bent shaft is encountered, the vibrations in the radial as well as in the axial direction will be high. Axial vibrations may be higher than the radial vibrations. The FFT will normally have 1× and 2× components. If the:

- Amplitude of 1× rpm is dominant then the bend is near the shaft center (Figure 5.7)
- Amplitude of 2× rpm is dominant then the bend is near the shaft end.

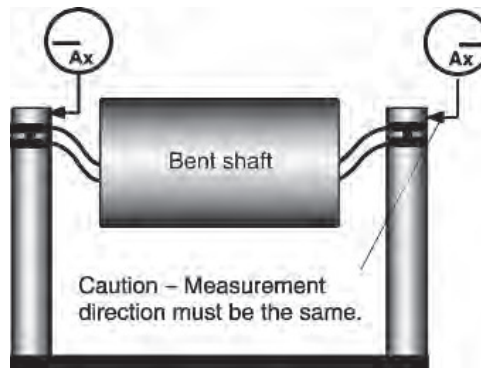


**Figure 5.7**  
*An FFT of a bent shaft with bend near the shaft center*

The phase will be 180° apart in the axial direction and in the radial direction. This means that when the probe is moved from vertical plane to horizontal plane, there will be no change in the phase reading (Figure 5.8).

### 5.2.4 Misalignment

Misalignment, just like unbalance, is a major cause of machinery vibration. Some machines have been incorporated with self-aligning bearings and flexible couplings that

**Figure 5.8**

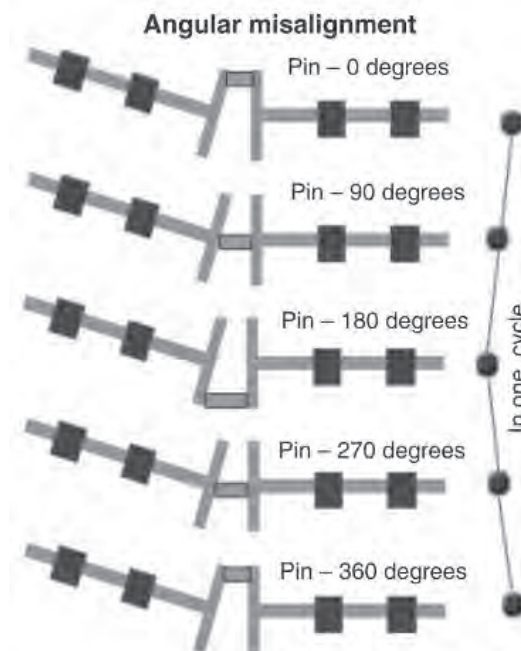
*Note the 180° phase difference in the axial direction*

can take quite a bit of misalignment. However, despite these, it is not uncommon to come across high vibrations due to misalignment. There are basically two types of misalignment:

1. *Angular misalignment*: the shaft centerline of the two shafts meets at angle with each other
2. *Parallel misalignment*: the shaft centerline of the two machines is parallel to each other and have an offset.

### Angular misalignment

As shown in Figure 5.9, angular misalignment primarily subjects the driver and driven machine shafts to axial vibrations at the  $1\times$  rpm frequency. The figure is an exaggerated and simplistic single-pin representation, but a pure angular misalignment on a machine is rare. Thus, misalignment is rarely seen just as  $1\times$  rpm peak. Typically, there will be high axial vibration with both  $1\times$  and  $2\times$  rpm. However, it is not unusual for  $1\times$ ,  $2\times$  or  $3\times$  to dominate. These symptoms may also indicate coupling problems (e.g. looseness) as well (Figure 5.10).

**Figure 5.9**

*Angular misalignment*

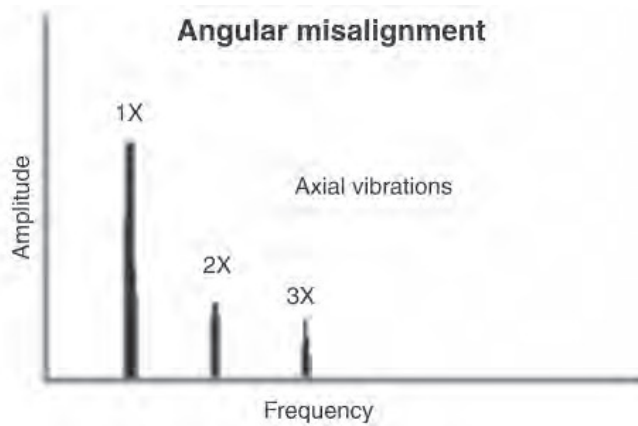


**Figure 5.10**  
*FFT of angular misalignment*

A  $180^\circ$  phase difference will be observed when measuring the axial phase on the bearings of the two machines across the coupling (Figure 5.11).

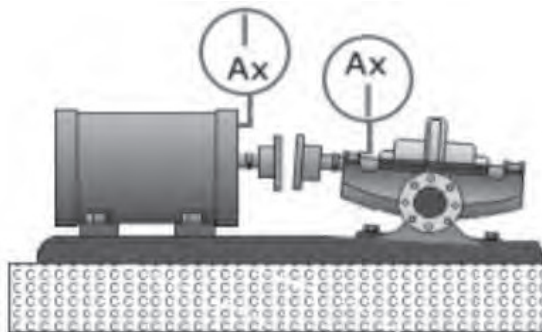


**Figure 5.11**  
*Angular misalignment confirmed by phase analysis*

### Parallel misalignment

Parallel misalignment, as shown in Figure 5.12, results in 2 *hits* per cycle and therefore a  $2\times$  rpm vibration in the radial direction. Parallel misalignment has similar vibration symptoms compared to angular misalignment, but shows high radial vibration that approaches a  $180^\circ$  phase difference across the coupling. As stated earlier, pure parallel misalignment is rare and is commonly observed to be in conjunction with angular misalignment. Thus, we will see both the  $1\times$  and  $2\times$  peaks. When the parallel misalignment is predominant,  $2\times$  is often larger than  $1\times$ , but its amplitude relative to  $1\times$  may often be dictated by the coupling type and its construction.

When either angular or parallel misalignment becomes severe, it can generate high-amplitude peaks at much higher harmonics ( $3\times$  to  $8\times$ ) (Figure 5.13) or even a whole series of high-frequency harmonics. Coupling construction will often significantly influence the shape of the spectrum if misalignment is severe (Figure 5.14).

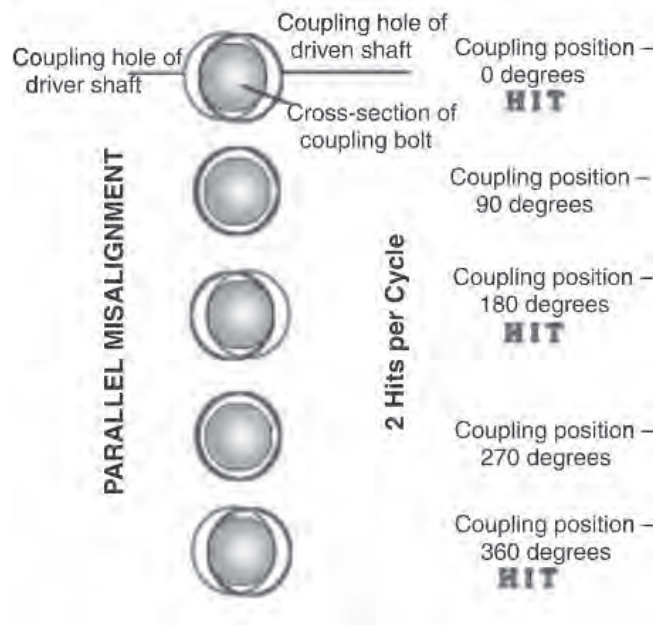


**Figure 5.12**  
*Parallel misalignment*

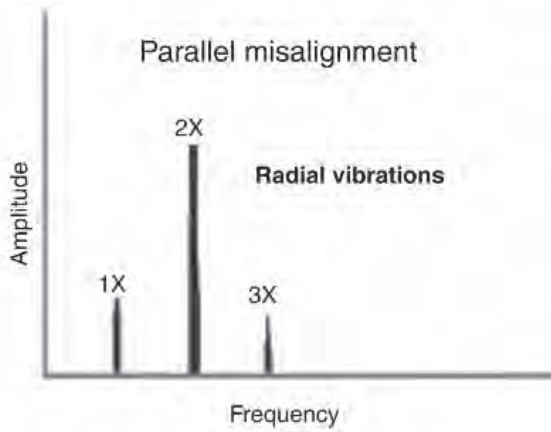


**Figure 5.13**  
*FFT of parallel misalignment*

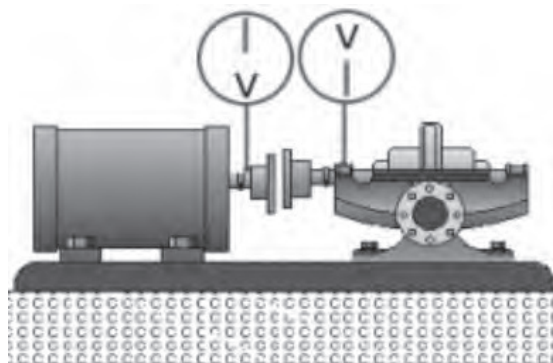


**Figure 5.14**  
*Radial phase shift of 180° is observed across the coupling*



An orbit is the trace of the shaft centerline for a single rotation. However, if we were to take an average position of the shaft centerline over a *certain* period of time, the result will describe something like what is shown on the left part of Figure 5.16. If the direction of rotation (DOR) of shaft is clockwise (CW) and if it is normally loaded, the ideal position of the average shaft centerline should be around the 7 o'clock to 8 o'clock position.

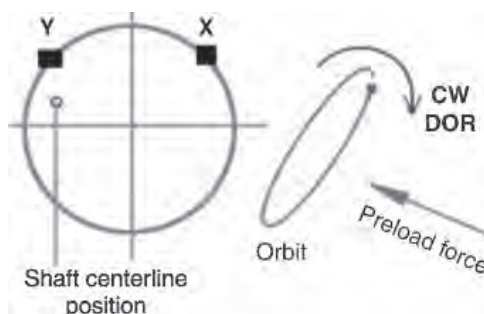


**Figure 5.16**  
*Orbit plot due to misalignment*

When radial preloads due to misalignment, gravity, fluid forces and other causes increase in magnitude, the orbit will become acutely ellipsoid. A bearing preload due to a cocked assembly can also cause the orbit to have lower amplitude in one axis that makes the ellipse look thinner. The average shaft centerline will move from the normal position to the upper left quadrant, for example.

In the figure, all points on the orbit are moving clockwise (which is the same as the direction of rotation) and therefore the orbit is still in *forward precession*. If the preloading increases further, it will result in the orbit's shape to resemble a number 8 character. In this case, it is also interesting to follow the average shaft centerline position, which has now moved further upwards into the left quadrant. If this orbit is carefully studied, it will be noticed that if a point on the orbit begins its journey from the *dot*, it is moving counter-clockwise initially, whereas the shaft is rotating in the clockwise direction. Thus, heavy preloading due to misalignment can cause the shaft to go into *reverse precession*. Forward precession is normal, reverse is not. If the trajectory of our imaginary point on the trace of the orbit is continued, one can visualize that precessions keep changing continuously (Figure 5.17).

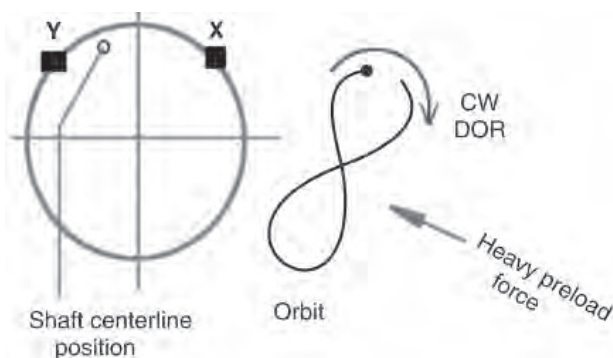


**Figure 5.17**  
*Orbit when the preload due to misalignment increase*

It should be noted that heavy preloads do not normally cause perfect number 8 orbits, but cause differently sized loops. This kind of loading, typically in a high-speed turbomachine, can be quite damaging and can result in excessive bearing wear, shaft fatigue and possibly shaft cracking.

## 5.2.5 Mechanical looseness

If we consider any rotating machine, mechanical looseness can occur at three locations:

1. Internal assembly looseness
2. Looseness at machine to base plate interface
3. Structure looseness.

### Internal assembly looseness

This category of looseness could be between a bearing liner in its cap, a sleeve or rolling element bearing, or an impeller on a shaft. It is normally caused by an improper fit between component parts, which will produce many harmonics in the FFT due to the non-linear response of the loose parts to the exciting forces from the rotor. A truncation of the time waveform occurs, causing harmonics. The phase is often unstable and can vary broadly from one measurement to the next, particularly if the rotor alters its position on the shaft from one start-up to the next.

Mechanical looseness is often highly directional and may cause noticeably different readings when they are taken at  $30^\circ$  increments in the radial direction all around the bearing housing. Also note that looseness will often cause sub-harmonic multiples at exactly  $\frac{1}{2} \times$  or  $\frac{1}{3} \times$  rpm (e.g.  $\frac{1}{2} \times$ ,  $1\frac{1}{2} \times$ ,  $2\frac{1}{2} \times$  and further) (Figures 5.18 and 5.19).

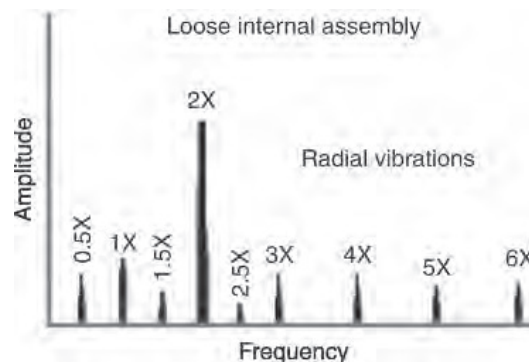


**Figure 5.18**  
*Loose internal assembly graph*

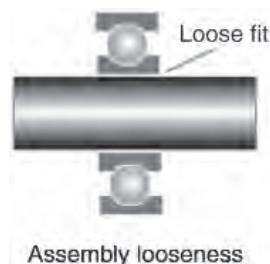


**Figure 5.19**  
*Loose fit*

### Looseness between machine to base plate

This problem is associated with loose pillow-block bolts, cracks in the frame structure or the bearing pedestal. Figures 5.20 and 5.21 make it evident how higher harmonics are generated due to the rocking motion of the pillow block with loose bolts.

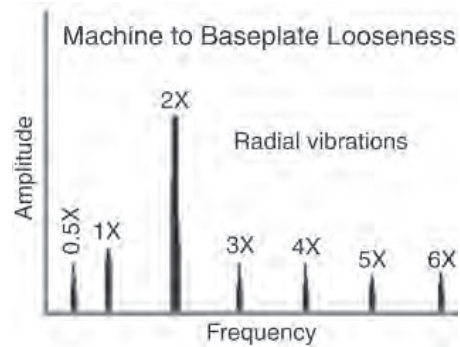


**Figure 5.20**  
*Mechanical looseness graph*

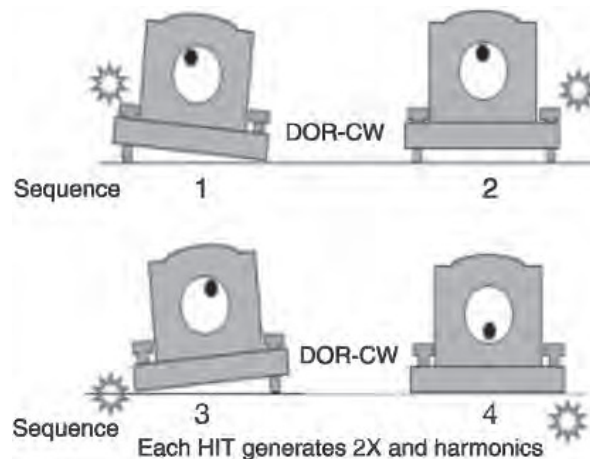


**Figure 5.21**  
*Mechanical looseness*

### Structure looseness

This type of looseness is caused by structural looseness or weaknesses in the machine's feet, baseplate or foundation. It can also be caused by deteriorated grouting, loose hold-down bolts at the base and distortion of the frame or base (known as 'soft foot') (Figure 5.22).

Phase analysis may reveal approximately 180° phase shift between vertical measurements on the machine's foot, baseplate and base itself (Figure 5.23).

When the soft foot condition is suspected, an easy test to confirm for it is to loosen each bolt, one at a time, and see if this brings about significant changes in the vibration. In this case, it might be necessary to re-machine the base or install shims to eliminate the distortion when the mounting bolts are tightened again.

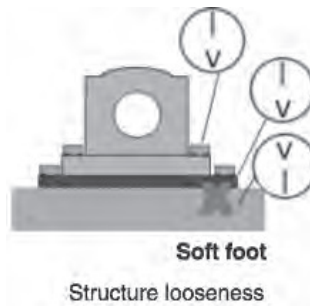


**Figure 5.22**  
Structure looseness

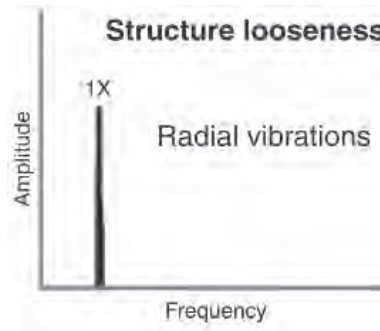


**Figure 5.23**  
Structure looseness graph

## 5.2.6 Resonance

Any object has a natural frequency which is determined by its characteristics of mass, stiffness and damping. If a gong strikes a bell, the bell rings at its own characteristic frequency known as its natural frequency. The gong-striking event is *forced vibration*, whereas the ringing of bell is *free vibration*.

A free vibration at a natural frequency is called resonance.

There is a simple method to find the natural frequency of any object or system called the *bump test*. With this method, a vibration sensor is fixed to the body whose natural frequency is required. Using an impact hammer, a blow is struck on the body and the time waveform or FFT is collected. The dominant frequency observed in the two graphs is the natural frequency of the body. Figures 5.24 and 5.25 show the time waveform and the FFT spectrum of a bump test conducted on a metal study table, respectively.

As seen in the time waveform, the impact occurs at approximately 100 ms after data collection was initiated. Directly after the impact, the body exhibits free vibrations at its own natural frequency. The amplitude of the vibration reduces logarithmically due to damping effects. The period between 500 ms and 1 s is long enough to count the number of cycles. The calculation indicates that the natural frequency is approximately 990 cpm. To obtain the FFT, the data collector was reset and another impact was made on the table with a hammer. The collected spectrum shows a dominant peak at 1046 cpm. This is close to the value calculated before with the time waveform.

The bump test is simple and used extensively in practice. It is a quick and accurate way of finding the resonance frequencies of structures and casings. It is tempting to use the bump test on a spare pump or other rotors not supported on bearings to obtain an estimate of their critical speeds. Take note that this can be very inaccurate. For example, the critical speed of rotors with impellers in a working fluid and supported by their bearings differs vastly from the critical speed obtained using a bump test off-line on the rotor.

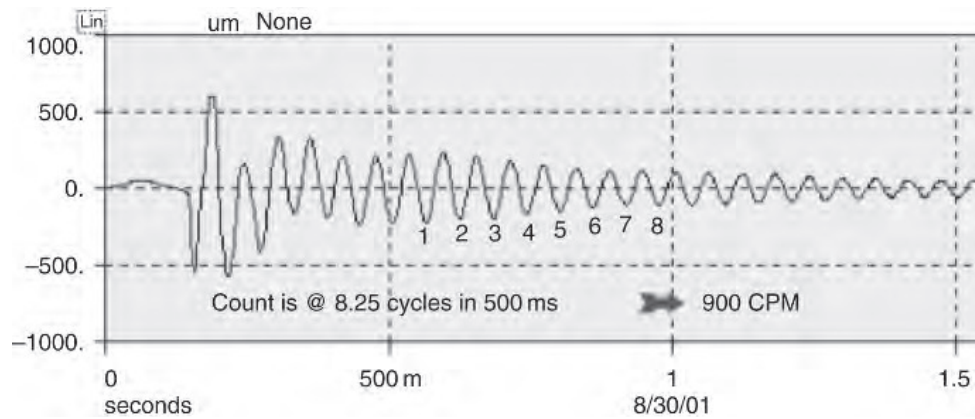


**Figure 5.24**  
Time waveform of a bump test

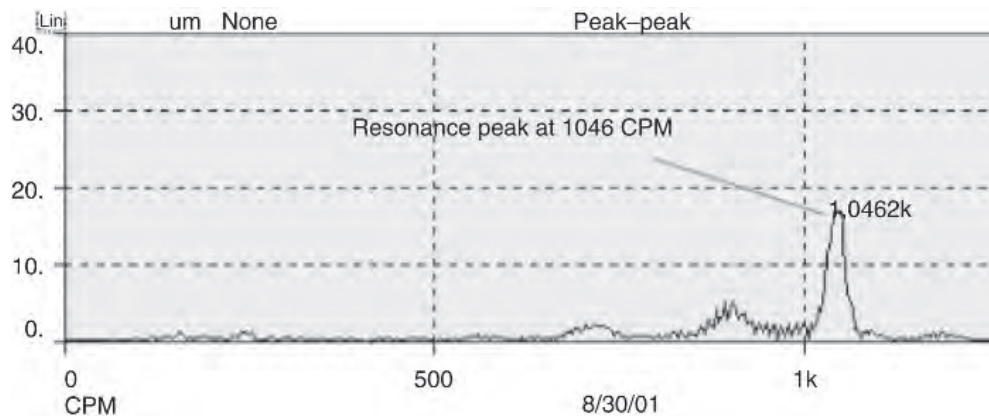


**Figure 5.25**  
FFT spectrum of a bump test

Assume that a multistage pump rotor has a natural frequency of 2500 cpm when pumping a fluid. Assume that the rotor has a slight unbalance, which generates tolerable amplitudes of vibration at  $1\times$  rpm. In this example, the unbalance causes the forced vibration frequency at  $1\times$  rpm. When the pump is started, the speed begins to increase and along with it also the amplitude and frequency of the vibration due to unbalance. At a particular instant, the forced frequency of vibration due to unbalance will be 2500 cpm. This frequency also happens to be the natural frequency of the rotor. Whenever the forced vibration frequency matches the natural frequency of a system, the amplitude rises significantly, much higher than expected compared to unbalance effects. This condition is called a *critical speed*.

Rotor critical speeds are confirmed using a Bode plot as shown in Figure 5.26. As the rotor approaches its critical speed, the amplitude rises. It reaches a maximum and then drops again. The phase changes steadily as well and the difference is  $90^\circ$  at the critical speed and nearly  $180^\circ$  when it passed through resonance.

The high-vibration amplitudes at critical speeds can be catastrophic for any system and must be avoided at all costs. Besides the example of the natural frequency of a rotor, structural resonance can also originate from support frame foundations, gearboxes or even drive belts.

Natural frequencies of a system cannot be eliminated, but can be shifted to some other frequency by various methods. Another characteristic of natural frequencies is that they remain the same regardless of speed, and this helps to facilitate their detection.

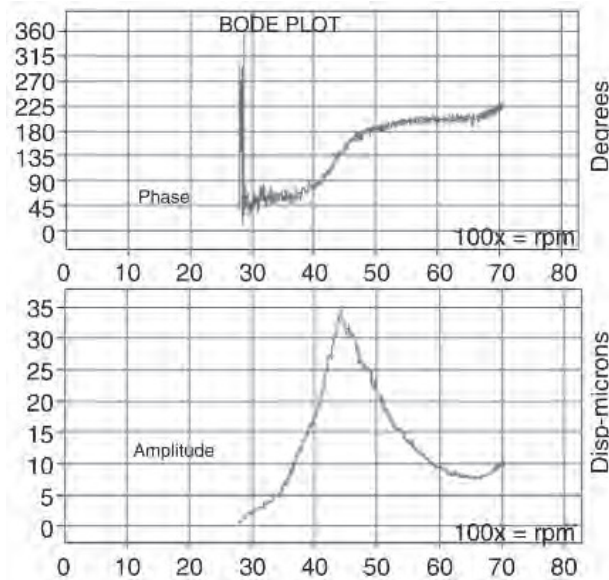


**Figure 5.26**  
*Rotor response represented by Bode plot*

To comprehend the reason for the shape of the Bode plot, we must go back to vibration basics. We have discussed earlier how the response of an object or mechanical system due to an exciting force such as unbalance can be represented as:

$$Mu \cdot r \cdot \omega^2 \cdot \sin(\omega t) = M(a) + C(v) + k(d)$$

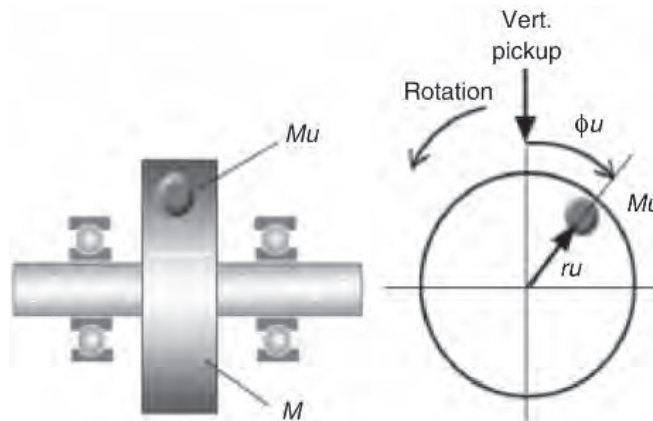


**Figure 5.27**  
*A simple rotor system*

Consider Figure 5.27, where:

- $M$  = rotor mass
- $Mr$  = unbalance mass
- $ru$  = radius of unbalance
- $\Phi_u$  = angular position of unbalance
- $\omega$  = angular velocity of rotor.

Figure 5.27 shows a simple rotor mass that is supported between two bearings. The mass  $M$  has an unbalanced mass  $Mr$  at a radius  $ru$  and at an angle  $\Phi u$  from the vertical sensor. If the rotor is forced to rotate, the synchronous response will be given by the equation:

$$Mr \cdot a + C \cdot v + K \cdot d = Mu \cdot ru \cdot \omega^2 \cdot \cos(\omega t - \Phi u)$$

The above equation in a vector format would appear graphically as shown in Figure 5.28. In this case, the exciting force is the unbalance force. The mass, damping and stiffness, which are the restraining forces add to a single force called the system force. In order to simplify this equation of motion, we replace acceleration with  $d \cdot \omega^2$  and velocity with  $d \cdot \omega$ .

The previous equation is now modified to:

$$(-Mr \cdot \omega^2 + C \cdot \omega + K) \cdot d = (Mu \cdot ru \cdot \omega^2) \cos(\omega t - \Phi u)$$

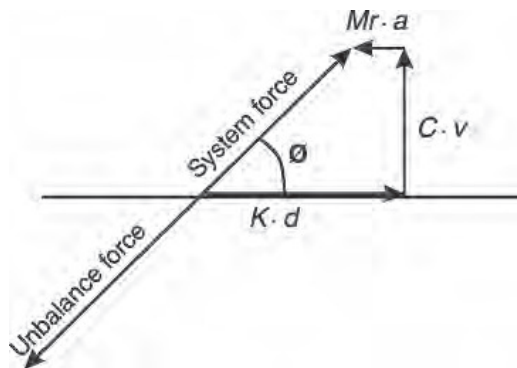


**Figure 5.28**  
System force-graph

Hence, with reference to Figures 5.29 and 5.30:

$$\text{synchronous dynamic stiffness} \times \text{displacement} = \text{unbalance force}$$

Rearranging the above equation we get:

$$\text{Synchronous response} = \frac{(M \cdot ru \cdot \omega^2)}{(-Mr \omega^2 + C \cdot \omega + k)}$$

$$\text{Synchronous response} = \frac{\text{unbalance force}}{\text{synchronous dynamic stiffness}}$$

**Figure 5.29**  
SDS Formulas

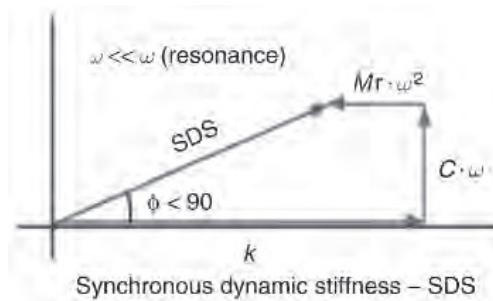


**Figure 5.30**  
SDS graph

Consequently, the synchronous response indicates that the  $1\times$  amplitude (displacement) increases when the unbalance force increases (or when the synchronous dynamic stiffness decreases).

We will now investigate the rotor response in the three speed ranges.

### Case 1 – Running speed $\omega$ is much less than critical speed

When the speed is less than the critical speed, the mass and damping contributions to stiffness are small. The dominant stiffness is the spring stiffness, which keeps the amplitudes low. At these low speeds, the unbalance force is changing and the spring stiffness is assumed not to be changing. The response of the rotor increases quadratic proportional to the speed (Figure 5.31).

The phase relationship of the rotor reference and the heavy spot is such that the vibration lags (phase difference =  $\phi$ ) behind the unbalance (heavy spot) and at this stage it is less than  $90^\circ$ .

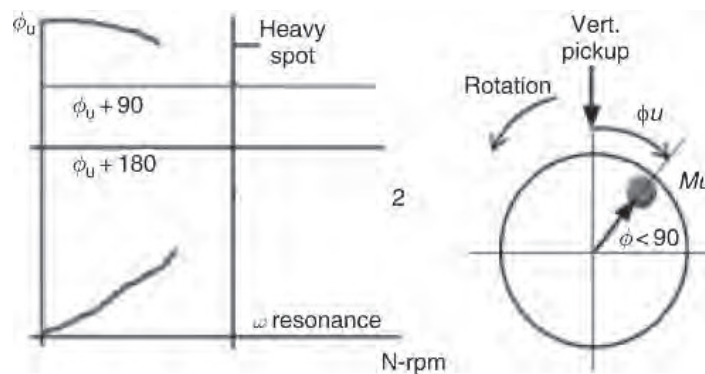


**Figure 5.31**  
Rotor response vs speed increase

### Case 2 – Running speed $\omega$ is equal to the critical speed (Figure 5.32)

When the rotor running speed approaches the critical speed, the mass stiffness and the spring stiffness contributions to the equation are equal in magnitude but opposite in direction. They thus cancel each other out and the only factor restraining the force is the damping. This is the reason why the synchronous rotor response (displacement at  $1\times$ ) is at its maximum at the critical speed.

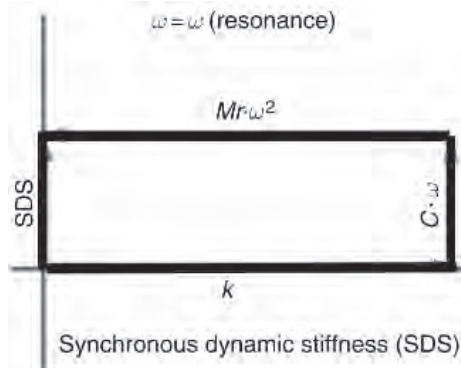


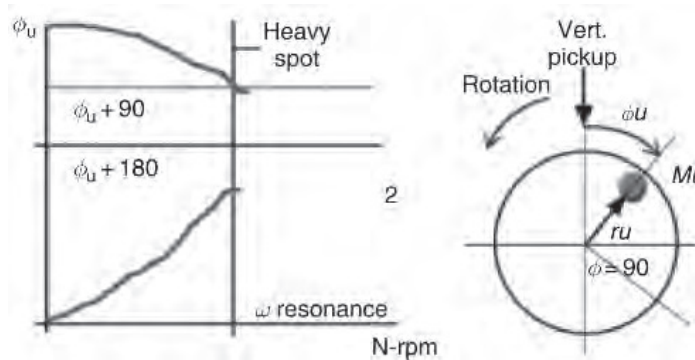
**Figure 5.32**  
Rotor speed reaches critical speed

The phase relationship between the response and the heavy spot is now exactly  $90^\circ$  (Figure 5.33). During critical speed we observe that the vectors:

$$k - M \cdot \omega^2 = 0$$

$$\therefore k = M \cdot \omega^2$$

Therefore the critical speed is:  $\omega = k/Mr$ .

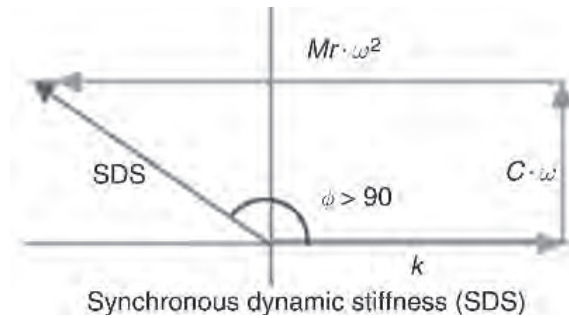


**Figure 5.33**  
Phase relationship at  $90^\circ$

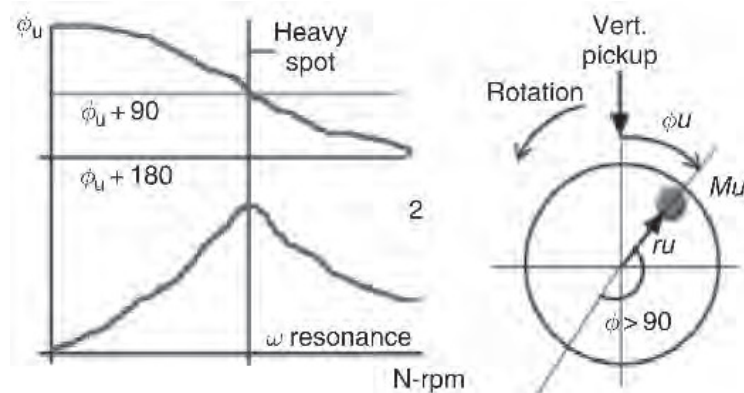
**Case 3 – running speed  $\omega$  greater than the critical speed**

As the speed increases beyond the critical speed, the mass stiffness contribution increases very rapidly (in quadratic proportion) and becomes higher in magnitude than the spring stiffness contribution, which almost remains the same in magnitude. The damping stiffness increases too but in linear proportion to the speed (Figure 5.34).

With the increase in synchronous dynamic stiffness, the amplitude of rotor vibration again drops, the phase difference continues to rise and by this stage it is close to  $180^\circ$ . This explains the nature of the Bode plot, which is a relationship of amplitude and phase vs running speed. The rising and falling of amplitude is due to the variations in the synchronous dynamic stiffness that changes at different speeds of the rotor (Figure 5.35).

**Figure 5.34**

At critical speeds, mass stiffness rises above spring stiffness

**Figure 5.35**

Dropping amplitude of rotor vibration

## 5.2.7 Rotor rubs

Rotor rubs produce a spectrum that is similar to mechanical looseness. A rub may be either partial or throughout the whole cycle. These generally generate a series of frequencies, and tend to excite one or more natural frequencies. Sometimes a phenomenon similar to chalk screeching on blackboard occurs during a rotor rub and it produces a white band noise on the spectrum in the high-frequency region. Normally the rub excites integer fractions of sub-harmonics of the running speed ( $\frac{1}{2}$ ,  $\frac{1}{3}$ ,  $\frac{1}{4}$  . . .  $\frac{1}{n}$ ), depending on the location of rotor natural frequencies.

The following relationships help to determine a rub. If  $N$  is the shaft speed and  $N_c$  is the critical speed of the shaft, then a rub will generate frequencies of:

$$\begin{aligned}
 &1\times && \text{when } N < N_c \\
 &\frac{1}{2}\times \text{ or } 1\times && \text{when } N > 2N_c \\
 &\frac{1}{3}\times, \frac{1}{2}\times \text{ or } 1\times && \text{when } N > 3N_c \\
 &\frac{1}{4}\times, \frac{1}{3}\times, \frac{1}{2}\times \text{ or } 1\times && \text{when } N > 4N_c
 \end{aligned}$$

A rub can have a short duration but can still be very serious if it is caused by the shaft touching a bearing (Figure 5.36). It is less serious when the shaft rubs a seal, an agitator blade rubs the wall of a vessel or a coupling guard presses against a shaft.

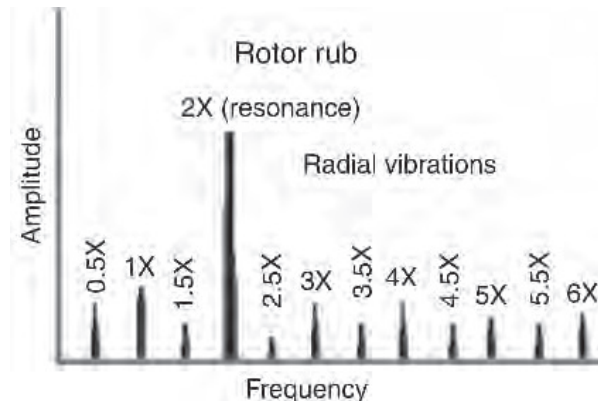


**Figure 5.36**  
*Rotor rub*

The waveform is a good indicator of a rub and it can get truncated as shown in Figure 5.37.

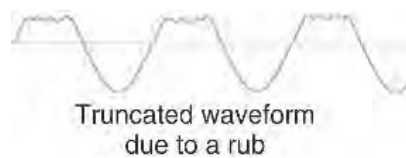


**Figure 5.37**  
*Truncated waveform*

### **Orbit representation of a rotor rub**

Orbit analysis is a good tool to identify rubs. As mentioned earlier, partial or complete rubs can occur when a rotating shaft comes in contact with stationary parts like seals or in abnormal cases of bearing (and/or instrumentation) failures. The rub causes the orbit to take on different shapes. From a number 8 to a full circle to something like the orbit shown in Figure 5.38.

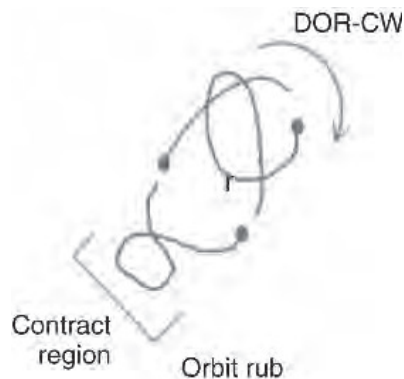


**Figure 5.38**  
*Orbit rub*

A partial rub is more common than a complete or a full annular rub and occurs when the rotor occasionally touches a stationary part. This normally generates a  $\frac{1}{2}\times$  vibration. The orbit may then look like a number 8 (as seen under the topic of *misalignment under severe preloading*), except that we can see two dots on the orbit. A full circle orbit may be indicative of a complete rub in which the rotor fully covers the seal or bearing clearance. In this case, the precession of vibration is observed to be in reverse and must hence be rectified immediately.

## 5.2.8 Journal bearings

### High clearance in journal bearings

Late stages of journal bearing wear normally display a whole series of running speed harmonics, which can be up to  $10\times$  or  $20\times$ . The FFT spectrum looks very much like that of mechanical looseness. Even minor unbalance or misalignment can cause higher vibration amplitudes compared with bearings having a normal clearance with the journal. This is due to a reduction in the oil film stiffness on account of higher clearances (Figure 5.39).

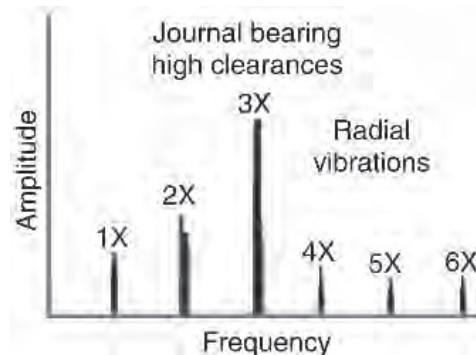


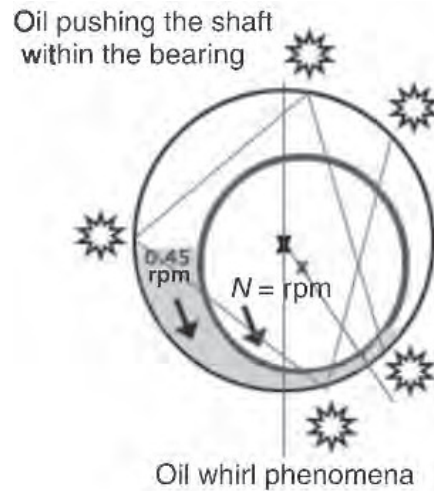
**Figure 5.39**  
*High clearance in journal bearings*

### Oil whirl

Oil whirl is an oil film-excited vibration. It is known to occur on machines equipped with pressure-lubricated journal bearings operating at high speeds (beyond their critical speed). Consider a shaft rotating in a bearing at speed  $N$ . The bearing speed is zero. The oil film is wedged between the shaft and the bearing and should ideally rotate at a speed of  $0.5\times$  rpm. However, some frictional losses cause the oil film to rotate at  $0.42\text{--}0.48\times$  rpm.

Under normal circumstances, the oil film pushes the rotor at an angle (5 o'clock if the shaft is rotating CCW – see Figure 5.40). An eccentric crescent-shaped wedge is created that has sufficient pressure to keep the rotor in the 'lifted' position. Under normal conditions, the system is in equilibrium and there are no vibrations.

Some conditions would tend to generate an oil film pressure in the wedge much higher than required to just hold the shaft. These conditions can cause an increase in bearing wear resulting in the shaft to have lower eccentricity (the shaft center is close to bearing center) causing a reduction in stiffness, oil pressure or a drop in oil temperature. In these cases, the oil film would push the rotor to another position in the shaft. The process continues over and over and the shaft keeps getting pushed around within the bearing. This phenomenon is called oil whirl. This whirl is inherently unstable since it increases centrifugal forces that will increase the whirl forces.

**Figure 5.40***Oil whirl*

Oil whirl can be minimized or eliminated by changing the oil velocity, lubrication pressure and external pre-loads. Oil whirl instability occurs at  $0.42\text{--}0.48\times$  rpm and is often quite severe. It is considered excessive when displacement amplitudes exceed 50% of the bearing clearances.

Oil whirl is basically a sub-synchronous fluid instability. When viewed in the orbit domain, it is shown with the characteristic two dots. When viewed with an oscilloscope, the two dots do not appear stationary, but seem to be rotating instead. This is because the frequency is marginally less than  $0.5\times$ . An oil whirl phenomenon generates a vibration precession, which is always forward (Figure 5.41).

**Figure 5.41***Orbit representation of an oil whirl*

## Oil whip

Oil whip can be caused when the shaft has no oil support, and can become unstable when the whirl frequency coincides with a critical speed. This special coincidence of shaft resonance coupled with the oil whirl frequency results in a more severe form of oil whirl called oil whip. Whirl speed will actually 'lock' onto the rotor critical speed and will not disappear even if the machine is brought to higher and higher speeds (Figure 5.42).

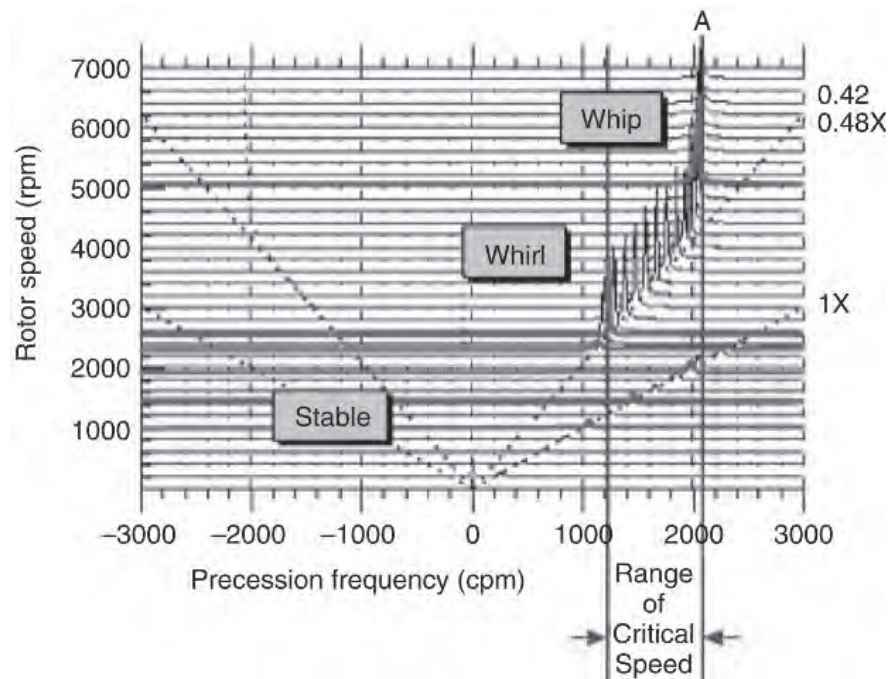


**Figure 5.42**

*Oil whirl/whip as seen in a cascade full spectrum – note the oil whip frequency ‘A’ getting locked even after raising rotor speed*

The oil whip phenomenon occurs when the rotor is passing through its critical speed. Oil whip is a destructive bearing defect. The precession of vibration is in the forward direction in this case, but some reverse  $1\times$  and sub-synchronous components are present due to anisotropy (changes in response when operating conditions change) of the bearing pedestal stiffness.

The period of this self-excited defect may, or might not, be harmonically related to the rotating speed of the shaft. When it is not harmonically related, the dots appear to be moving randomly as shown in Figure 5.43. When it is harmonically related they appear stationary.



**Figure 5.43**

*Orbit representation of an oil whirl*

### Dry whirl

Sometimes inadequate or improper lubrication can also cause vibrations in a bearing. This is because lack of lubrication results in friction between the shaft and the bearing. The friction force will also tend to excite other parts of the machine. This vibration is

similar to the experience of moving a moist finger over a glass pane. The vibration caused by this phenomenon is known as dry whirl. The vibration is generally at high frequencies, and harmonics may not be present. Phase will not provide any meaningful information.

## 5.2.9 Rolling element bearings

A rolling element bearing comprises of inner and outer races, a cage and rolling elements. Defects can occur in any of the parts of the bearing and will cause high-frequency vibrations. In fact, the severity of the wear keeps changing the vibration pattern. In most cases, it is possible to identify the component of the bearing that is defective due to the specific vibration frequencies that are excited. Raceways and rolling element defects are easily detected. However, the same cannot be said for the defects that crop up in bearing cages. Though there are many techniques available to detect where defects are occurring, there are no established techniques to predict when the bearing defect will turn into a functional failure.

In an earlier topic dealing with enveloping/demodulation, we saw how bearing defects generate both the bearing defect frequency and the ringing random vibrations that are the resonant frequencies of the bearing components.

Bearing defect frequencies are not integrally harmonic to running speed. However, the following formulas are used to determine bearing defect frequencies. There is also a bearing database available in the form of commercial software that readily provides the values upon entering the requisite bearing number.

$$BPFI = \frac{Nb}{2} \left(1 + \frac{Bd}{Pd} \cos \theta\right) \times \text{rpm}$$

$$BPFO = \frac{Nb}{2} \left(1 - \frac{Bd}{Pd} \cos \theta\right) \times \text{rpm}$$

$$FTF = \frac{1}{2} \left(1 - \frac{Bd}{Pd} \cos \theta\right) \times \text{rpm}$$

$$BSF = \frac{Pd}{2Bd} \left[1 - \left(\frac{Bd}{Pd}\right)^2 (\cos \theta)^2\right] \times \text{rpm}$$

Nb = Number of Balls or Rollers

Bd = Ball / Roller diameter (inch or mm)

Pd = Bearing pitch diameter (inch or mm)

$\theta$  = Contact angle in degrees

BPFI = Ball pass frequency – Inner

BPFO = Ball pass frequency – Outer

FTF = Fundamental train frequency (Cage)

BSF = Ball spin frequency (rolling element)

It is very interesting to note that in an FFT, we find both the inner and outer race defect frequencies. Add these frequencies and then divide the result by the machine rpm – [(BPFI + BPFO)/rpm]. The answer should yield the number of rolling elements.

Bearing deterioration progresses through four stages. During the initial stage, it is just a high-frequency vibration, after which bearing resonance frequencies are observed. During the third stage, discrete frequencies can be seen, and in the final stage high-frequency random noise is observed, which keeps broadening and rising in average amplitude with increased fault severity.

## Stage 1 of bearing defect

The FFT spectrum for bearing defects can be split into four zones (A, B, C and D), where we will note the changes as bearing wear progresses. These zones are described as:

- Zone A: machine rpm and harmonics zone
- Zone B: bearing defect frequencies zone (5–30 kcpm)
- Zone C: bearing component natural frequencies zone (30–120 kcpm)
- Zone D: high-frequency-detection (HFD) zone (beyond 120 kcpm).

The first indications of bearing wear show up in the ultrasonic frequency ranges from approximately 20–60 kHz (120–360 kcpm). These are frequencies that are evaluated by high-frequency detection techniques such as gSE (Spike Energy), SEE, PeakVue, SPM and others.

As Figure 5.44 shows, the raceways or rolling elements of the bearing do not have any visible defects during the first stage. The raceways may no longer have the shine of a new bearing and may appear dull gray.

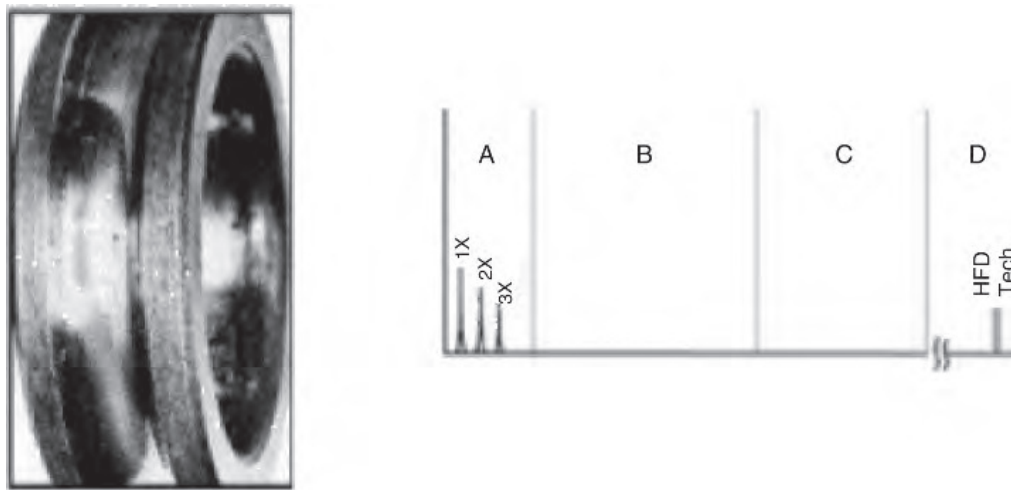


**Figure 5.44**  
*Small defects in the raceways of a bearing*

## Stage 2 of bearing defect

In the following stage (Figure 5.45), the fatigued raceways begin to develop minute pits. Rolling elements passing over these pits start to generate the ringing or the bearing component natural frequencies that predominantly occur in the 30–120 kcpm range. Depending on the severity, it is possible that the sideband frequencies (bearing defect frequency  $\pm$  rpm) appear above and below the natural frequency peak at the end of stage two. The high-frequency detection (HFD) techniques may double in amplitude compared to the readings during stage one.

## Stage 3 of bearing defect

As we enter the third stage (Figure 5.46), the discrete bearing frequencies and harmonics are visible in the FFT. These may appear with a number of sidebands. Wear is usually now visible on the bearing and may expand through to the edge of the bearing raceway.

The minute pits of the earlier stage are now developing into bigger pits and their numbers also increase. When well-formed sidebands accompany any bearing defect frequency or its harmonics, the HFD components have again almost doubled compared to stage three. It is usually advised to replace the bearing at this stage. Some studies indicate that after the third stage, the remaining bearing life can be 1 h to 1% of its average life.

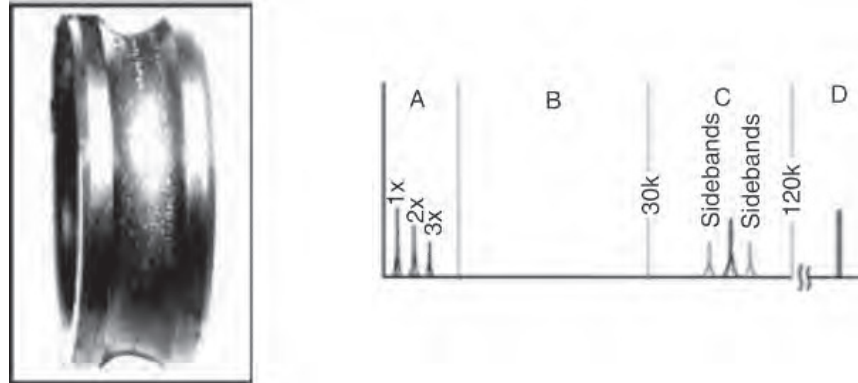


**Figure 5.45**  
*More obvious wear in the form of pits*

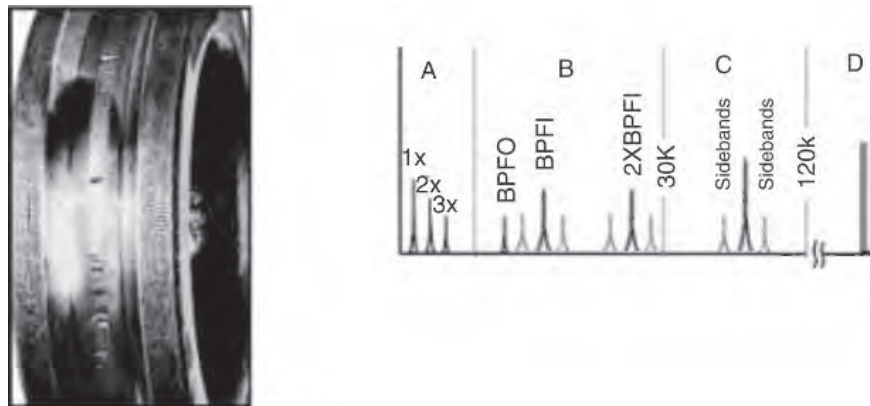


**Figure 5.46**  
*Wear is now clearly visible over the breadth of the bearing*

#### **Stage 4 of bearing defect**

In the final phase (Figure 5.47), the pits merge with each other, creating rough tracks and spalling of the bearing raceways or/and rolling elements. The bearing is in a severely damaged condition now. Even the amplitude of the 1× rpm component will rise. As it grows, it may also cause growth of many running speed harmonics. It can be visualized as higher clearances in the bearings allowing a higher displacement of the rotor.

Discrete bearing defect frequencies and bearing component natural frequencies actually begin to merge into a random, broadband high-frequency ‘noise floor’. Initially, the average amplitude of the broad noise may be large. However, it will drop and the width of the noise will increase. In the final stage, the amplitude will rise again and the span of the noise floor also increases.

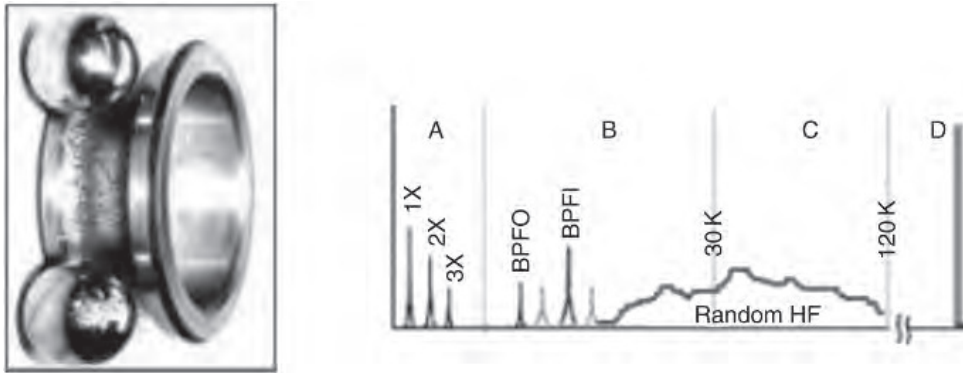


**Figure 5.47**  
*Severely damaged bearing in final stage of wear*

However, amplitudes of the high-frequency noise floor and some of the HFD may in fact decrease (due to pits flattening to become spalls), but just prior to failure spike energy will usually grow to extreme amplitudes.

By this time, the bearing will be vibrating excessively; it will be hot and making lots of noise. If it is allowed to run further, the cage will break and the rolling elements will go loose. The elements may then run into each other, twisting, turning and welded to one another, until the machine will hopefully trip on overload. In all probability, there will be serious damage to the shaft area under the bearing.

### 5.2.10 Gearing defects

A gearbox is a piece of rotating equipment that can cause the normal low-frequency harmonics in the vibration spectrum, but also show a lot of activity in the high-frequency region due to gear teeth and bearing impacts. The spectrum of any gearbox shows the 1× and 2× rpm, along with the gear mesh frequency (GMF). The GMF is calculated by the product of the number of teeth of a pinion or a gear, and its respective running speed:

$$\text{GMF} = \text{number of teeth on pinion} \times \text{pinion rpm}$$

The GMF will have running speed sidebands relative to the shaft speed to which the gear is attached. Gearbox spectrums contain a range of frequencies due to the different GMFs and their harmonics. All peaks have low amplitudes and no natural gear frequencies are excited if the gearbox is still in a good condition. Sidebands around the GMF and its harmonics are quite common. These contain information about gearbox faults (Figure 5.48).

Tooth wear and backlash can excite gear natural frequencies along with the gear mesh frequencies and their sidebands. Signal enhancement analysis enables the collection of vibrations from a single shaft inside a gearbox.

Cepstrum analysis is an excellent tool for analysing the power in each sideband family. The use of cepstrum analysis in conjunction with order analysis and time domain averaging can eliminate the ‘smearing’ of the many frequency components due to small speed variations (Figure 5.49).

As a general rule, distributed faults such as eccentricity and gear misalignment will produce sidebands and harmonics that have high amplitude close to the tooth-mesh frequency. Localized faults such as a cracked tooth produce sidebands that are spread more widely across the spectrum.

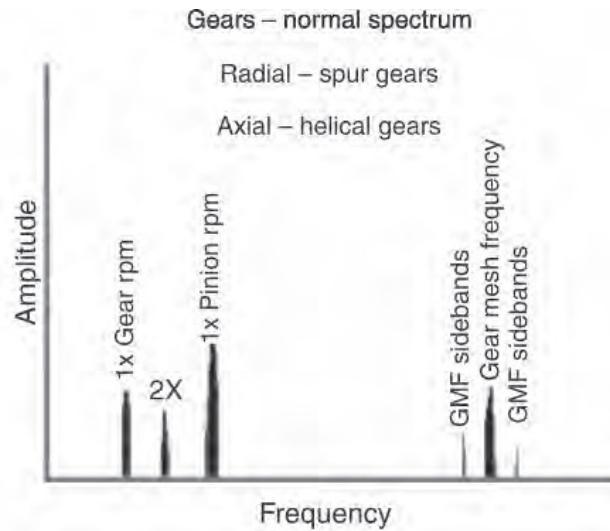


**Figure 5.48**  
*Graph of a gearbox spectrum*

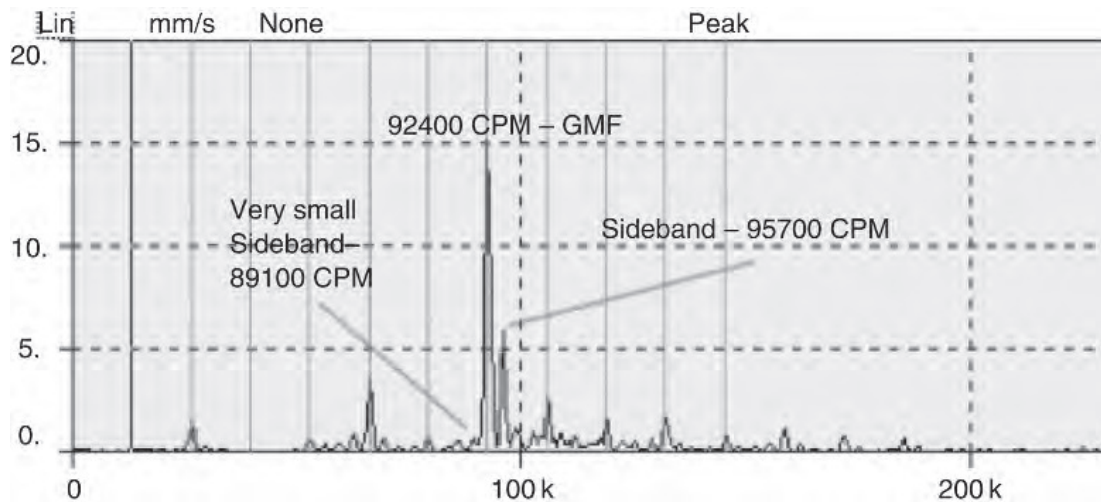


**Figure 5.49**  
*FFT spectrum from a noisy gearbox with pinion having 28 teeth and rotating at 3300 rpm*

### **Gear tooth wear**

An important characteristic of gear tooth wear is that gear natural frequencies are excited with sidebands around them. These are spaced with the running speed of the bad gear. The GMF may or may not change in amplitude, although high-amplitude sidebands surrounding the GMF usually occur when wear is present. Sidebands are a better wear indicator than the GMF itself (Figure 5.50).

### **Gear tooth load**

As the load on a gearbox increases, the GMF amplitude may also increase. High GMF amplitudes do not necessarily indicate a problem, particularly if sideband frequencies remain low and no gear natural frequencies are excited. It is advised that vibration analysis on a gearbox be conducted when the gearbox is transmitting maximum power (Figure 5.51).

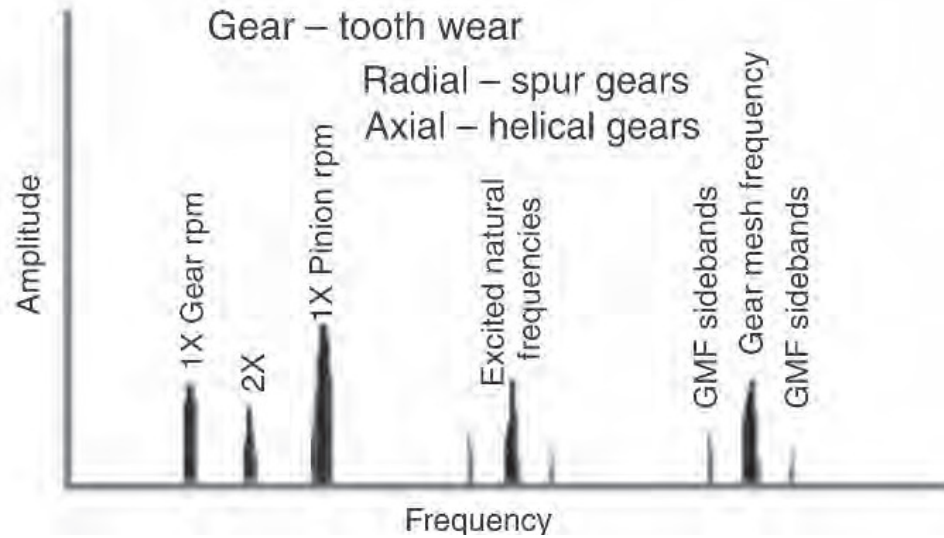


**Figure 5.50**  
Gear tooth wear

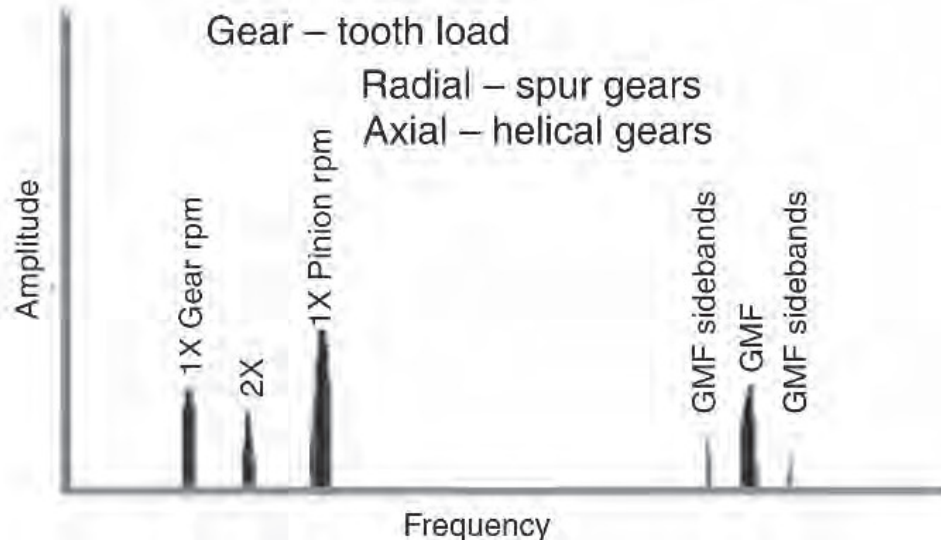


**Figure 5.51**  
Gear tooth load

### Gear eccentricity and backlash

Fairly high amplitude sidebands around the GMF often suggest gear eccentricity, backlash or non-parallel shafts. In these cases, the rotation of one gear may cause the amplitude of gear vibration to *modulate* at the running speed of the other. This can be seen in the time domain waveform. The spacing of the sideband frequencies indicates the gear with the problem. Improper backlash normally excites the GMF and gear natural frequencies. Both will have sidebands at  $1\times$  rpm. The GMF amplitudes will often decrease with increasing load if backlash is the problem (Figure 5.52).

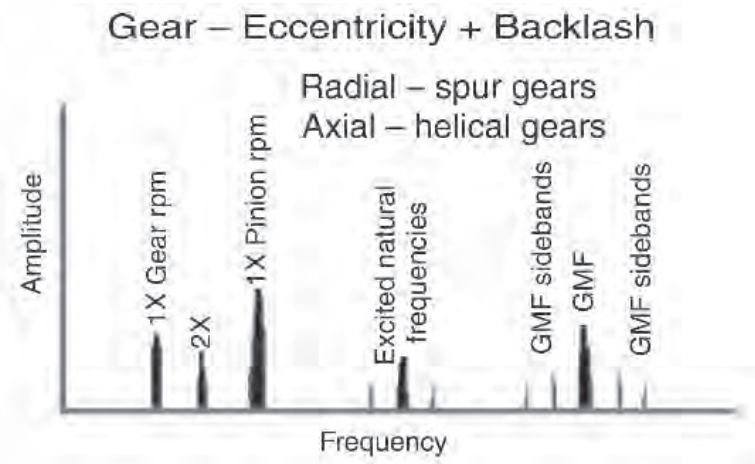


**Figure 5.52**  
*Gear eccentricity and backlash*

### **Gear misalignment**

Gear misalignment almost always excites second order or higher GMF harmonics, which will have sidebands spaced with the running speed. It will often show only small amplitudes at  $1\times$  GMF, but much higher levels at  $2\times$  or  $3\times$  GMF. It is important to set the F-max of the FFT spectrum to more than  $3\times$  GMF (Figure 5.53).

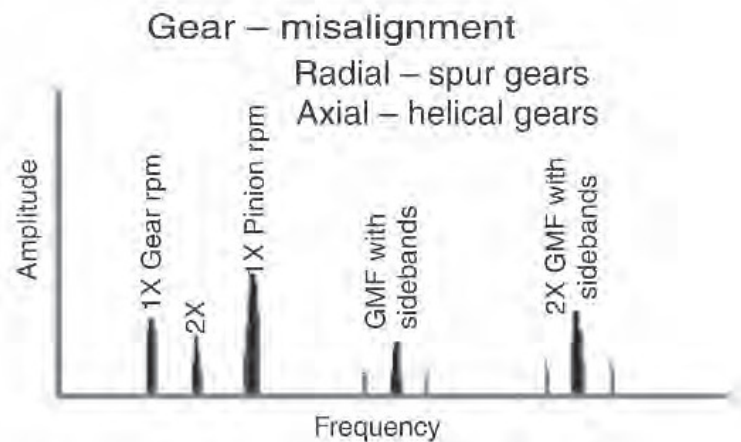


**Figure 5.53**  
*Gear misalignment*

### **Gears – cracked or broken tooth**

A cracked or broken gear tooth will generate high amplitude at  $1\times$  rpm of this gear, plus it will excite the gear natural frequency with sidebands spaced with its running speed. It is best detected in the time domain, which will show a pronounced spike every time the problematic tooth tries to mesh with teeth on the mating gear. The time between impacts will correspond to  $1/\text{speed}$  of the gear with the broken tooth. The amplitude the impact spike in the time waveform will often be much higher than that of the  $1\times$  gear rpm in the FFT spectrum (Figure 5.54).

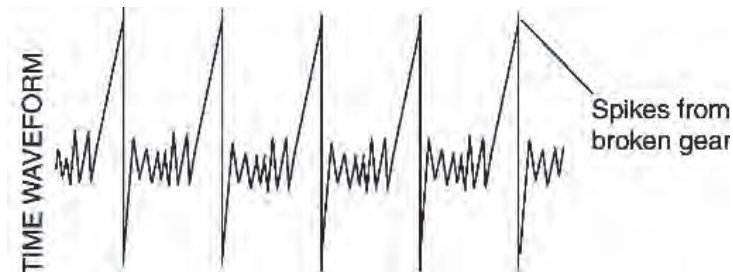


**Figure 5.54**  
*Gears – cracked*

### Gears – hunting tooth problems

The gear hunting tooth frequency is particularly effective for detecting faults on both the gear and the pinion that might have occurred during the manufacturing process or due to mishandling. It can cause quite high vibrations, but since it occurs at low frequencies, predominantly less than 600 cpm, it is often missed during vibration analysis. The hunting tooth frequency is calculated with:

$$\text{Hunting Tooth Frequency} = \frac{\text{GMF} \times N}{(\text{no. of pinion teeth}) \times (\text{no. of gear teeth})}$$

In the above equation,  $N$  is known as the *assembly phase factor*, also referred to as the lowest common integer multiple between the number of teeth on the pinion and gear. This hunting tooth frequency is usually very low.

For assembly phase factors ( $N > 1$ ), every gear tooth will not mesh with every pinion tooth. If  $N = 3$ , teeth numbers 1, 4, 7, etc. will mesh with one another (however, gear tooth 1 will not mesh with pinion teeth 2 or 3; instead, it will mesh with 1, 4, 7, etc.). For example, a gear with 98 teeth is running at 5528 rpm and is meshing with a pinion with 65 teeth and running 8334 rpm. The assembly phase factor is  $N = 1$ . The hunting tooth frequency (Fht) can be calculated as follows:

$$\text{Fht} = \frac{(98 \times 5528) \times 1}{98 \times 65} = 85 \text{ cpm (1.42 Hz)}$$

Another formula is the rpm of the gear divided by the number of pinion teeth ( $5528/65 = 85$  cpm). This is a special case and applies to a hunting tooth combination only when  $N = 1$ .

If the tooth repeat frequency is a problem (Figure 5.55), one can usually audibly hear it since it is a beat frequency. A gearset with a tooth repeat problem normally emits a ‘growling’ sound from the driven end. Its repetition rate can often be established by simply counting the sounds using a stopwatch. The maximum effect occurs when the faulty pinion and gear teeth mesh at the same time (on some drives, this may occur once every 10 or 20 revolutions, depending on the Fht formula).

Gearboxes can generate crowded and complex FFT spectrums with many unusual and unidentifiable frequencies. Another unusual frequency encountered in the gearbox is a sub-multiple of the gear mesh frequency. This vibration is generally the result of an eccentric gear shaft misalignment or possibly a bent shaft. Any one of these cases can cause variations in the tooth clearances for each revolution of the

gear. As a result, the amplitude of the gear mesh frequency may appear modulated as shown in Figure 5.56.

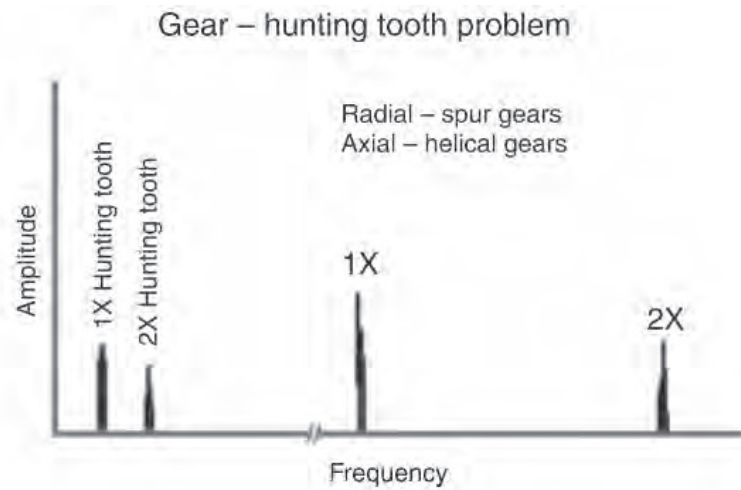


**Figure 5.55**  
*Gear – hunting tooth problem*

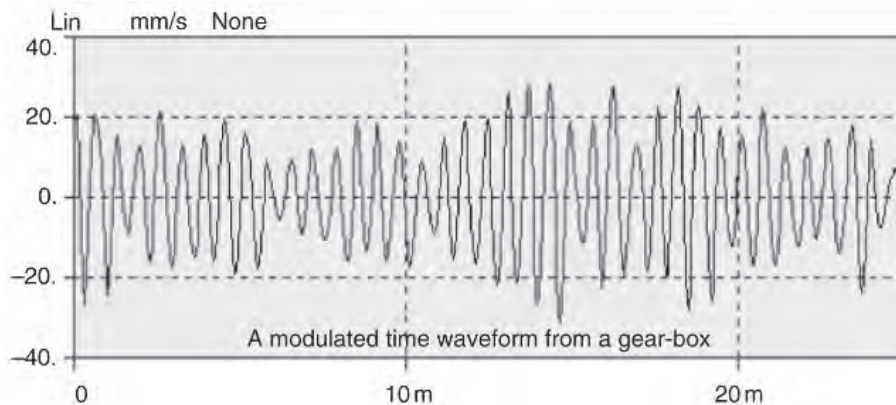


**Figure 5.56**  
*Modulated amplitude from a gearbox with a GMF of 92400 cpm*

Gear tooth impacts may only be excessive during portions of each revolution of the gear. Therefore the resulting vibration will have a frequency less than the gear mesh frequency. However, it will remain a multiple of the gear rpm.

## 5.2.11 Belt defects

### Worn, loose, mismatched belts

Belt defect frequencies are of the sub-harmonic type. Upon analysing belt drives, it is necessary to keep the F-max low to be able to notice these peaks. When belts are worn, loose or mismatched, they may generate harmonics of the belt frequency. It is possible to

obtain 3× or 4× times of belt frequency. Quite often, the 2× belt frequency is dominant. The belt frequency (Figure 5.57) is given by the formula:

$$\text{Belt frequency} = \frac{\pi \times \text{pulley rpm} \times \text{pitch dia.}}{\text{belt length}}$$

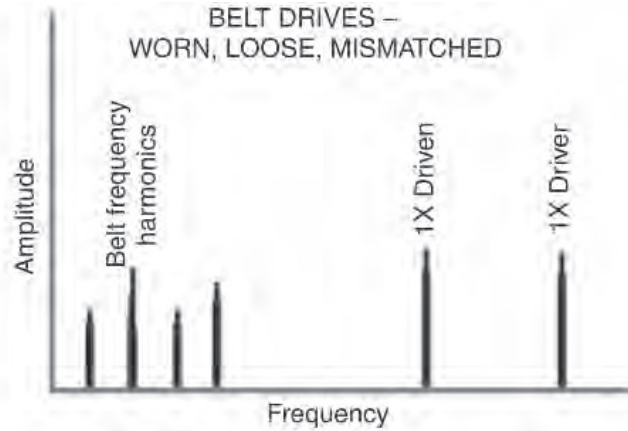


**Figure 5.57**  
*Sub-harmonic belt frequencies*

Amplitudes are normally unsteady, sometimes pulsing with either driver or driven rpm. With timing belt drives, it is useful to know that high amplitudes at the timing belt frequency indicate wear or pulley misalignment.

### Belt/sheave misalignment

The different types of misalignment possible with belt drives are shown in Figure 5.58. These conditions not only result in destructive vibration but also cause accelerated wear of both the belt and the sheaves. Misalignment of sheaves produces high vibration at 1× rpm, predominantly in the axial direction (Figure 5.59). The ratio of amplitudes of driver to driven rpm depends on the measurement position, relative mass and the frame stiffness. With sheave misalignment in fans, the highest axial vibration will be at the fan rpm. When the belt drives an overhung rotor, which is in an unbalanced condition, it will have to be resolved with phase analysis.

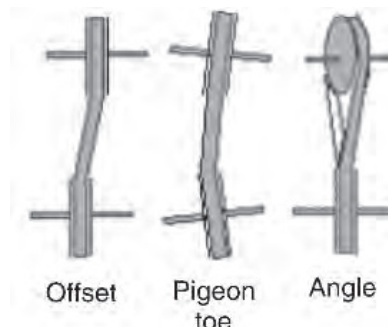


**Figure 5.58**  
*Misalignment types (the pigeon toe and angle are classified as angular misalignment)*

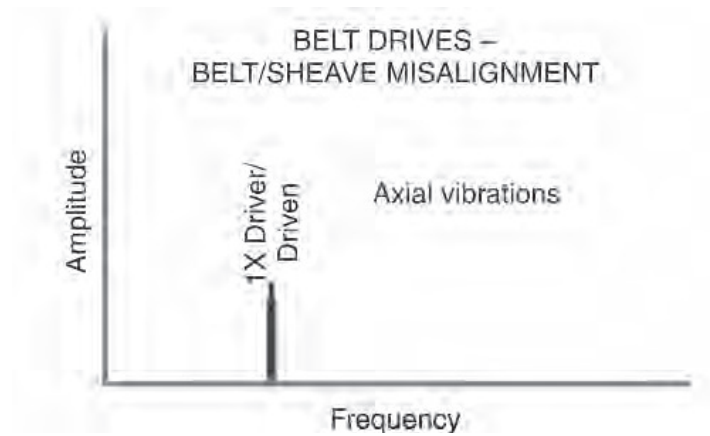


**Figure 5.59**  
*Vibration due to sheave misalignment*

### **Eccentric sheaves**

Eccentric or unbalanced sheaves cause maximum vibration at  $1\times$  rpm of the sheave, causing problems in line with the sheaves. To resolve this condition, it may sometimes be possible to balance eccentric sheaves by attaching washers to taperlock bolts. However, even if balanced, the eccentricity will still induce vibration and cause fatigue stresses in the belt (Figure 5.60).

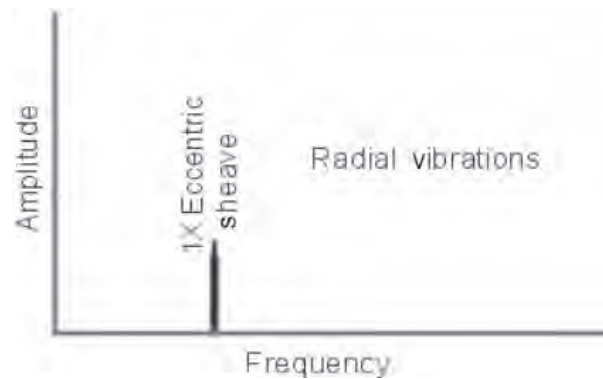


**Figure 5.60**  
*Belt drives – eccentric sheaves*

### **Belt resonance**

Belt resonance (Figure 5.61) can occur if the natural frequency of the belt is close to either the motor or the driven shaft rpm. Drive belts also experience high vertical and lateral vibrations when their natural frequencies coincide with that of connected equipment. Tensioning and releasing the belt while measuring the response on sheaves or bearings can normally identify and help to rectify this situation.

A common method to control vertical vibration is by using a restraining device (metal rod or idler pulley) placed perpendicular to the belt span and close to (or lightly touching) the belt. This device should be positioned roughly at one-third of the span distance from the larger pulley.

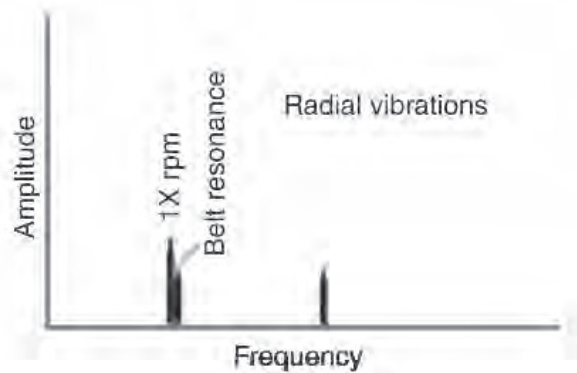


**Figure 5.61**  
Belt drives – resonance

Other alternatives to reduce the amplitude of vibration or alter the belt resonance frequency are to modify the span length, belt type, alignment, inertia of driving or driven machinery, pulley diameter and weight, speed, and the number of belts.

### 5.2.12 Electrical problems

Vibrations of electrical machines such as motors, generators and alternators can be either mechanical or electrical in nature. We have discussed most common mechanical problems. Electrical problems also appear in the vibration spectrum and can provide information about the nature of the defects. Electrical problems occur due to unequal magnetic forces acting on the rotor or the stator. These unequal magnetic forces may be due to:

- Open or short windings of rotor or stator
- Broken rotor bar
- Unbalanced phases
- Unequal air gaps.

Generally, the vibration pattern emerging due to the above-mentioned electrical problems will be at  $1\times$  rpm and will thus appear similar to unbalance.

A customary technique to identify these conditions is to keep the analyzer capturing the FFT spectrum in the *live* mode and then switching off the electrical power. If the peak disappears instantly, the source is electrical in nature. On the other hand, if there is gradual decrease in the  $1\times$  amplitude it is more likely to be a mechanical problem. This technique requires caution. If there is a time lag in the analyzer itself, it may delay the drop in vibration amplitude. It is also possible that a resonance frequency may drop quickly as the speed changes.

Induction motors, which have electrical problems, will cause the vibration amplitude to hunt or swing in a cyclic manner. The phase readings will show similar cycles too. Under a stroboscope, the reference mark will move back and forth.

The swinging amplitudes in induction motor applications are due to two dominant frequencies that are very close to one another. They continuously add and subtract to one another in a phenomenon known as *beats*. It can also possibly be a single frequency whose amplitude is modulating.

In fact, hunting amplitudes are the first indication of a possible electrical problem in the motor. Understanding the nature of these vibrations can assist in identifying the exact

defects in an electrical machine. The following are some terms that will be required to understand vibrations due to electrical problems:

$F_L$  = electrical line frequency (50/60 Hz)

$F_s$  = slip frequency =  $\frac{2 \times F_L}{P}$  - rpm

$F_p$  = pole pass frequency =  $F_s \times P$

$P$  = number of poles.

### **Rotor problems**

Normally, four kinds of problems can occur within the rotor:

1. Broken rotor bars
2. Open or shorted rotor windings
3. Bowed rotor
4. Eccentric rotor.

### **Rotor defects**

Along with the stator is a rotor, which is basically an iron following the rotating magnetic field. As the magnetic field sweeps across the conductor, it creates a voltage across the length of the rotor bar. If the bar is open-circuited, no current flows and no forces are generated. When the bar is short-circuited, a current flows. This current is proportional to the speed at which the field cuts through the conductor and the strength of the field. The field interacts with the stator field to generate a force on the rotor bar. If everything else remains the same, an equal and opposite force on the opposite side of the rotor will develop. These two forces generate the torque that drives the load. In case anything disrupts the current or magnetic fields on either side of the rotor, the two forces will become unequal. This results in a radial force, which is the cause for vibration.

A cracked or broken bar can cause this category of unbalanced forces. The forces rotate with the rotor with a constant load plus a load that varies with  $2 \times$  slip. Therefore, the force acting on the bearings will have frequency components at  $1 \times$  rpm and  $1 \times$  rpm  $\pm 2 \times$  slip. Thus:

- Broken or cracked rotor bars or shorting rings (Figures 5.62 and 5.63)
- Bad joints between rotor bars and shorting rings
- Shorted rotor laminations

will produce high  $1 \times$  running speed vibration with pole pass frequency sidebands. In addition, cracked rotor bars will often generate  $F_p$  sidebands around the 3rd, 4th and 5th running speed harmonics.

Loose rotor bars are indicated by  $2 \times$  line frequency ( $2F_L$ ) sidebands surrounding the rotor bar pass frequency (RBPF) and/or its harmonics (Figure 5.64).

$$\text{RBPF} = \text{number of rotor bars} \times \text{rpm}$$

It may often cause high levels at  $2 \times$  RBPF with only a small amplitude at  $1 \times$  RBPF.

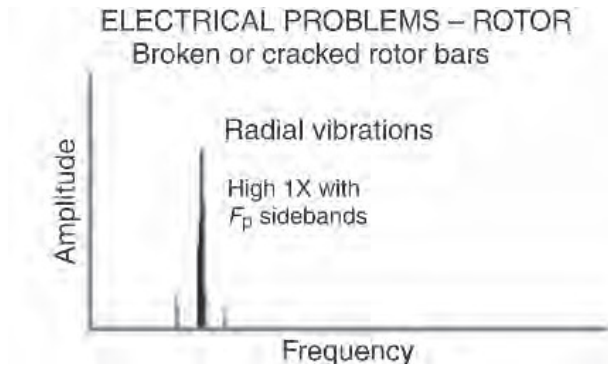


**Figure 5.62**  
*High 1X with  $F_p$  sidebands*

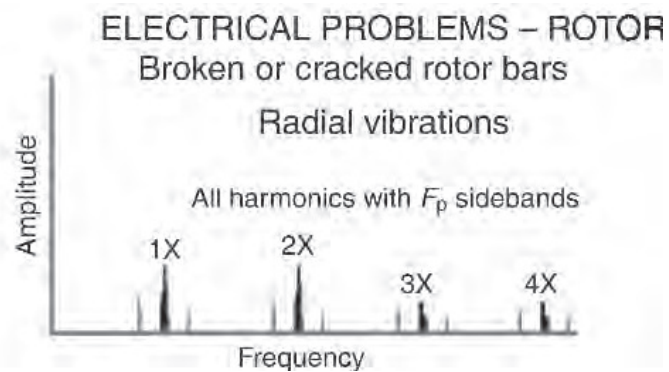


**Figure 5.63**  
*All harmonics with  $F_p$  sidebands*

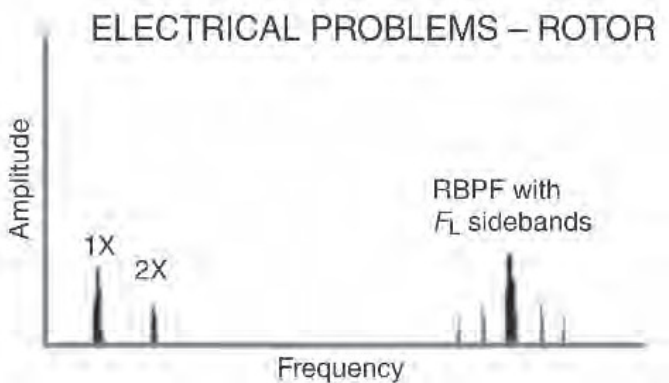


**Figure 5.64**  
*Rotor bar pass frequency*

**Eccentric rotor**

The rotor is supposed to be concentric with respect to the stator coils. If this is not the case, a magnetic unbalance force is generated which is given by the formula:

$$F = \frac{KI^2}{g^2} \left( \frac{4e}{(1-e)^2} \right)$$

where  $I$  = stator current,  $g$  = average gap between stator and rotor,  $e$  = eccentricity.

From this equation, it can be observed that an increase in current and eccentricity can generate high unbalanced magnetic forces. It is assumed that the eccentricity of the rotor will line up with the magnetic field. The closer side of the rotor will be respectively attracted to the positive pole and to the negative pole; thus the force will vary twice during a single current cycle. This can affect the bearings, and therefore it can modulate any other frequency present in the system.

These effects generally cause sidebands of  $\pm 2 \times$  slip frequency around the  $1 \times$  rpm frequency caused by unbalance. Eccentric rotors produce a rotating variable air gap between the rotor and stator, which induces pulsating vibrations (it is a beat phenomenon between two frequencies, one is  $2F_L$  and is the closest running speed harmonic). This may require a 'zoom' spectrum to separate the  $2F_L$  and the running speed harmonic.

Eccentric rotors generate  $2F_L$  surrounded by pole pass frequency sidebands ( $F_P$  as well as  $F_P$  sidebands around  $1 \times$  rpm). The pole pass frequency  $F_P$  itself appears at a low frequency (Figure 5.65).

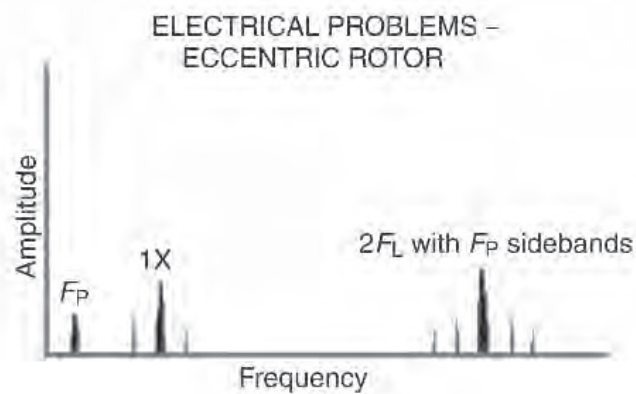


**Figure 5.65**  
Eccentric rotor

### Stator defects

An induction motor comprises a set of stator coils, which generate a rotating magnetic field. The magnetic field causes alternating forces in the stator. If there is any looseness or a support weakness in the stator, each pole pass gives it a tug. This generates a  $2 \times$  line frequency ( $2F_L$ ) also known as *loose iron*. Shorted stator laminations cause uneven and localized heating, which can significantly grow with time (Figure 5.66).

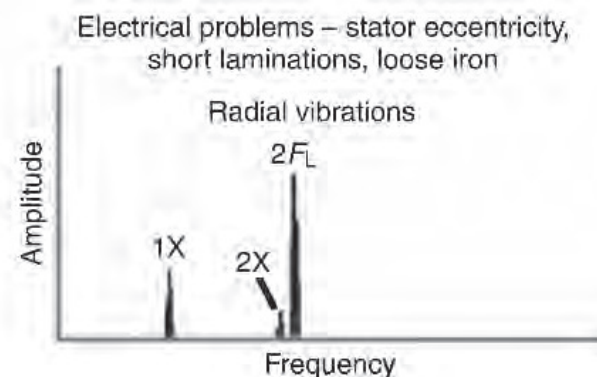


**Figure 5.66**  
Stator defects

Stator problems generate high vibration at  $2F_L$ . Eccentricity produces uneven stationary air gaps between the rotor and the stator, which produce very directional vibration. Differential air gaps should not exceed 5% for induction motors and 10% for synchronous motors. Soft foot and warped bases can generate an eccentric stator.

### Phasing problem (loose connector)

Phasing problems due to loose or broken connectors can cause excessive vibration at  $2F_L$ , which will have sidebands around it spaced at  $\frac{1}{3}$  rd of the line frequency ( $\frac{1}{3} F_L$ ). Levels at  $2F_L$  can exceed 25 mm/s (1.0 in./s) if left uncorrected. This is particularly a problem if the defective connector is sporadically making contact and not periodically (Figure 5.67).

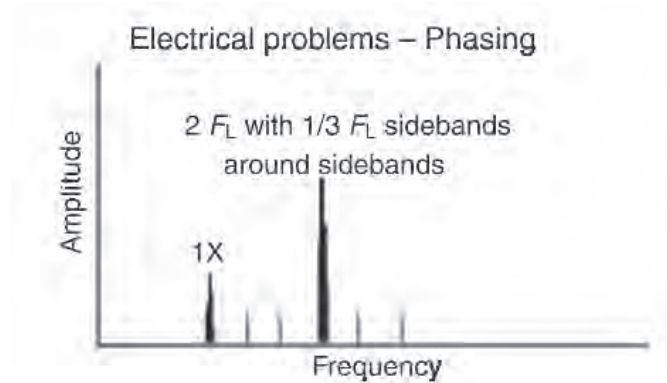


**Figure 5.67**  
*Phasing problem*

### Synchronous motors (loose stator coils)

Loose stator coils in synchronous motors will generate fairly high vibrations at the coil pass frequency (CPF), defined as:

$$\text{CPF} = \text{number of stator coils} \times \text{rpm}$$

(number of stator coils = poles  $\times$  number of coils/pole)

The coil pass frequency will be surrounded by 1 $\times$  rpm sidebands (Figure 5.68).

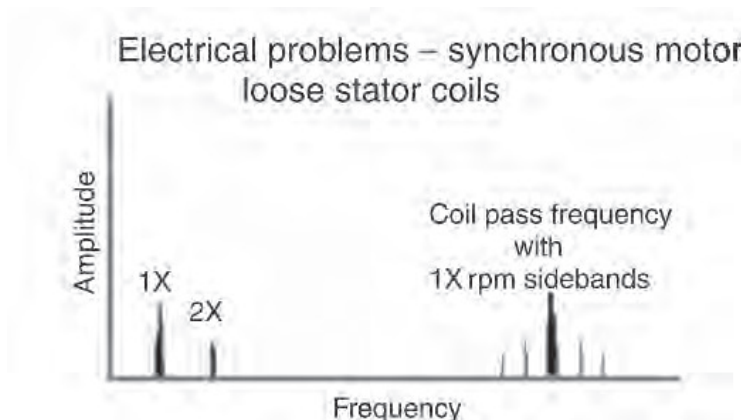


**Figure 5.68**  
*Synchronous motors*

## DC motor problems

DC motor defects can be detected by high vibration amplitudes at the SCR firing frequency ( $6F_L$ ) and harmonics. These defects include broken field windings, bad SCRs and loose connections (Figure 5.69).

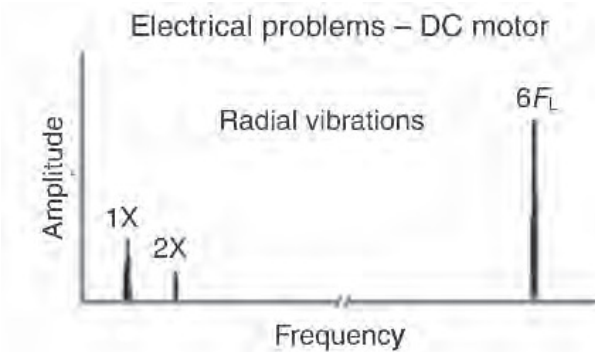


**Figure 5.69**  
*DC Motor*

Other defects, such as loose or blown fuses and shorted control cards, can cause high amplitude peaks at  $1\times$  through  $5\times$  line frequency.

### 5.2.13 Flow-related vibrations

#### Blade pass and vane pass vibrations

Blade pass or vane pass frequencies (Figure 5.70) are characteristics of pumps and fans. Usually it is not destructive in itself, but can generate a lot of noise and vibration that can be the source of bearing failure and wear of machine components.

$$\text{Blade pass frequency (BPF)} = \text{number of blades (or vanes)} \times \text{rpm}$$

This frequency is generated mainly due to the gap problems between the rotor and the stator. A large amplitude BPF (and its harmonics) can be generated in the pump if the gap between the rotating vanes and the stationary diffusers is not kept equal all the way around.

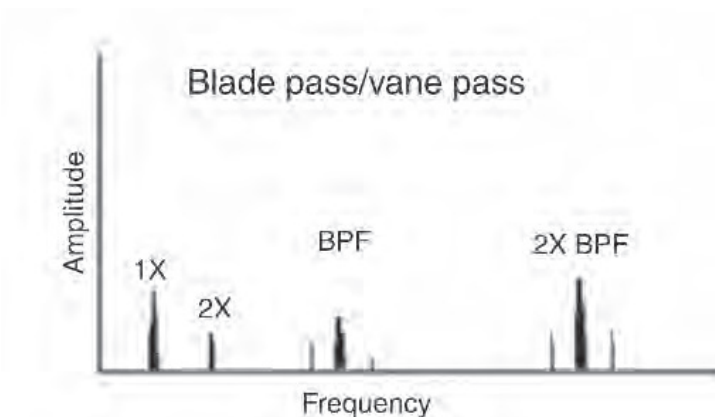


**Figure 5.70**  
*Blade pass/vane pass*

In centrifugal pumps, the gap between the impeller tip and the volute tongue or the diffuser inlet is a certain percentage (in the region of 4–6% of the impeller diameter), depending on the speed of the pump. If the gap is less than the recommended value, it can generate a noise that resembles cavitation. However, an FFT plot will immediately highlight the vane pass frequency of the impeller. Also, the BPF (or its harmonics) sometimes coincides with a system natural frequency, causing high vibrations.

A high BPF can be generated if the wear ring seizes on the shaft or if the welds that fasten the diffusers fail. In addition, a high BPF can be caused by abrupt bends in linework (or duct), obstructions which disturb the flow path, or if the pump or fan rotor is positioned eccentrically within the housing.

Similar to the vane pass frequency, centrifugal pumps are known to generate non-specific sub-synchronous or even supersynchronous (larger than 1×) discrete frequencies. These are rare occurrences, but in all probability they transpire in two-stage (or higher) pumps, which have intermediate bushes that act as additional stiffness components. An increase in the clearances within these bushes leads to a fall in stiffness and this results in enlarged vibrations.

In a two-stage overhung impeller pump, the interstage bushing plays an important role in providing stiffness, which is described as the Lomakin effect. When clearances are high, this effect can reduce and high amplitude supersynchronous frequencies are generated. Once the clearances are adjusted back to normal, the pump operation stabilizes and the defect frequency disappears.

### Flow turbulence

Flow turbulence (Figure 5.71) often occurs in blowers due to variations in pressure or velocity of the air passing through the fan or connected linework. In fans, duct-induced vibration due to stack length, ductwork turns, unusual fan inlet configuration and other factors may be a source of low-frequency excitation. This flow disruption causes turbulence, which will generate random, low-frequency vibrations, typically in the range of 20–2000 cpm.

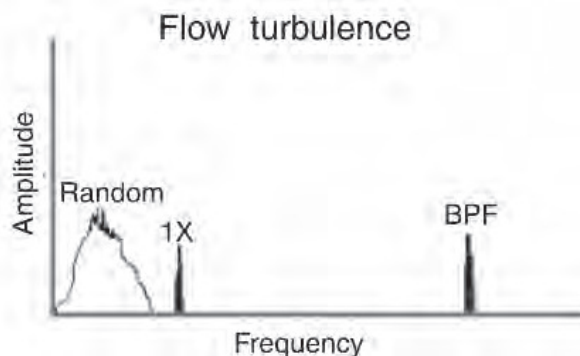


**Figure 5.71**  
*Flow turbulence*

*Rotating stall* is one of the flow-induced vibrations that can occur in fans and compressors. Rotating stall is a flow separation of the fluid from the blades under certain low-flow conditions. Rotating stall sometimes occur in a system with a partially closed inlet damper. The condition usually appears as a low sub-synchronous frequency

component in the rotor vibration spectrum (frequency ratios are typically between 8 and 40%, but can be as high as 80% of the rotational speed).

From a diagnostics point of view, rotating stall differs from the other whirl category instabilities due to its strong dependence on the *operating conditions*. Normally, correcting the operating flow makes it disappear. It differs from surge because it is proportional to the running speed of the fan or compressor. Surging is in the axial direction, which is not the case with rotating stall. Rotating stall manifests in the rotor vibration spectrum with sub-synchronous frequencies, which tracks the rotor speed. The orbit will have a forward precession.

In pumps, flow turbulence induces vortices and wakes in the clearance space between the impeller vane tips and the diffuser or volute lips. Dynamic pressure fluctuations or pulsation produced in this way can result in shaft vibrations because the pressure pulses impinge on the impeller.

Flow past a restriction in pipe can produce turbulence or flow-induced vibrations. The pulsation could produce noise and vibration over a wide frequency range. The frequencies are related to the flow velocity and geometry of the obstruction. These in turn excite resonant frequencies in other pipe components. The shearing action produces vortices that are converted to pressure disturbances at the pipe wall, which may cause localized vibration excitation of the pipe or its components.

It has been observed that vortex flow is even higher when a system's acoustic resonance coincides with the generated frequency from the source. The vortices produce broadband turbulent energy centered around the frequency determined by the following formula:

$$f = \frac{S_n \times V}{D}$$

where  $f$  = vortex frequency (Hz),  $S_n$  = Strouhl number (dimensionless, between 0.2 and 0.5),  $D$  = characteristic dimension of the obstruction.

For example, a liquid flowing at 35 m/s past a 6-in. stub line would produce broadband turbulence at frequencies from 40 to 100 Hz.

## **Cavitation**

Cavitation normally generates random, high-frequency broadband energy, which is sometimes superimposed with the blade pass frequency harmonics. Gases under pressure can dissolve in a liquid. When the pressure is reduced, they bubble out of the liquid.

In a similar way, when liquid is sucked into a pump, the liquid's pressure drops. Under conditions when the reduced pressure approaches the vapor pressure of the liquid (even at low temperatures), it causes the liquid to vaporize. As these vapor bubbles travel further into the impeller, the pressure rises again causing the bubbles to collapse or implode.

This implosion has the potential to disturb the pump performance and cause damage to the pump's internal components. This phenomenon is called *cavitation*. Each implosion of a bubble generates a kind of impact, which tends to generate high-frequency random vibrations (Figure 5.72).

Cavitation can be quite destructive to internal pump components if left uncorrected. It is often responsible for the erosion of impeller vanes. Cavitation often sounds like 'gravel' passing through the pump. Measurements to detect cavitation are usually not taken on bearing housings, but rather on the suction piping or pump casing.

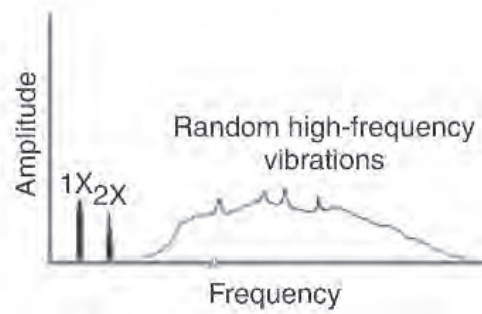


**Figure 5.72**  
*Cavitation*

Cavitation is best recognized by observing the complex wave or dynamic pressure variation using an oscilloscope and a pressure transducer. The pressure waveform is not sinusoidal, and the maximum amplitudes appear as sharp spikes. Between these spikes are low amplitude, smooth and rounded peaks.

### 5.2.14 Rotor crack

The basic principle during crack development is that the rotor loses stiffness in the direction perpendicular to the crack direction. Imagine a flat steel ruler. Tie a heavy weight to one end of the ruler with the help of a string. As we turn the ruler, we see a big deflection when the broad and flat surface is on top. When it is turned through  $90^\circ$ , the thin section of the ruler is on top and this time we hardly notice any deflection.

Thus, in one revolution of the ruler we will see two big deflections, and in two instances there will be almost zero deflection. The two big deflections per revolution would cause the  $2\times$  rpm vibration frequency.

This same principle applies to a shaft under a heavy side load, such as a turbine rotor acting under gravity. If a crack develops on the circumference of a rotor, transverse to the shaft axis, the stiffness in the plane perpendicular to the crack decreases and remains the same in the other orthogonal plane (Figure 5.73).

This is similar to the flat steel ruler example, and therefore we will observe an analogous phenomenon. To diagnose this fault properly, we must look at all the information obtained from the vibration amplitude and the phase data carefully.

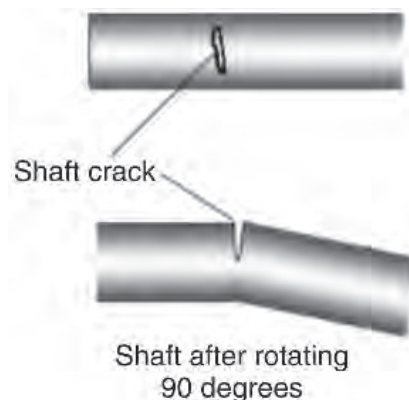


**Figure 5.73**  
*Shaft crack*

There are two fundamental symptoms of a shaft crack:

1. Unexplained changes in the  $1\times$  shaft relative amplitude and phase
2. Occurrence of a  $2\times$  rpm vibration frequency.

The first vital symptom is the changes in the  $1\times$  synchronous amplitude and phase. On a turbomachine installed with proximity probes measuring shaft vibration, it may also be possible to notice the defect on a slow roll bow vector (at a low rotational speed).

Shaft bending due to a transverse crack causes the changes in the synchronous  $1\times$  amplitude and phase. It is important to note that the amplitude and phase could be higher or even lower. Thus, any change in the  $1\times$  amplitude and phase should cause an alarm for the possibility of this defect.

The next classical symptom is the occurrence of the  $2\times$  rpm component. The cause for this component (as explained earlier) is due to asymmetry in the horizontal shaft stiffness on which radial forces like gravity may be acting. When viewed on a cascade plot, during a startup or coastdown, the  $2\times$  frequency is especially dominant when the rotational speed is in the region of half the critical speed.

When the speed is increased, this  $2\times$  peak diminishes. When the rotor crosses the critical speed, the  $2\times$  amplitude also rises along with  $3\times$  and  $4\times$  components that may also be present. When the rotor reaches full speed, the high  $1\times$  may be accompanied by this  $2\times$  frequency too.

Although this is a transient observation, the  $1\times$  amplitude and phase can be monitored under normal operating conditions as well to provide alarms and early warnings of a possible shaft crack. A polar plot (Figure 5.74) provides a good format for highlighting the change in the  $1\times$  amplitude and phase.

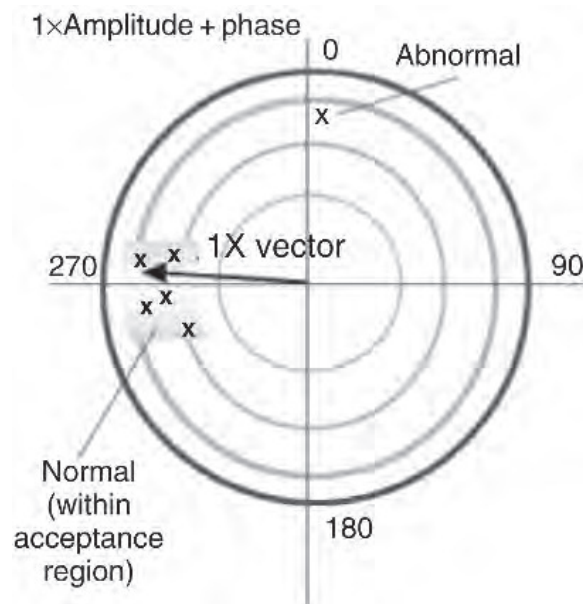


**Figure 5.74**  
*Polar plot*

A region in the form of a sector can be plotted to indicate the normal operating vector position that describes the  $1\times$  amplitude and phase. These are also called *acceptance regions*. Acceptance regions can also be plotted for the  $2\times$  component during the transient analysis to provide evidence of a shaft crack.

Any change in the position of this vector will cause it to move away from the sector. Alarm windows can be created around this sector to draw attention to a deviation.

It should be kept in mind that many other factors such as load, field current, steam conditions or other operating parameters could have changed and might be causing the changes in the  $1\times$  and  $2\times$  amplitude and phase readings. A thermal blow in a large steam turbine can cause a similar high  $1\times$  component. Misalignment can cause large  $1\times$  and  $2\times$  components. In some cases, the high  $1\times$  amplitude was associated with unbalance. However, if a shaft cannot be balanced properly, a crack could be the culprit.